Thermal conductivity in one-dimensional electronic fluids

D. B. Gutman,[1,a)] I. V. Protopopov,[2] R. Samanta,[3] and A. D. Mirlin[4,5]

AFFILIATIONS

[1]Department of Physics, Bar Ilan University, Ramat Gan 52900, Israel
[2]Department of Theoretical Physics, University of Geneva, Geneva 1211, Switzerland
[3]Birla Institute of Technology and Science, Pilani, Hyderabad 500078, India
[4]Institute for Quantum Materials and Technologies, Karlsruhe Institute of Technology, Karlsruhe 76021, Germany
[5]Institute for Condensed Matter Theory, Karlsruhe Institute of Technology, Karlsruhe 76128, Germany

[a)]**Author to whom correspondence should be addressed:** Dmitri.Gutman@biu.ac.il

ABSTRACT
We study thermal conductivity in one-dimensional electronic fluids combining kinetic [R. Samanta, I. V. Protopopov, A. D. Mirlin, and D. B. Gutman, Thermal transport in one-dimensional electronic fluid, Phys. Rev. Lett. 122, 206801 (2019)] and hydrodynamic [I. V. Protopopov, R. Samanta, A. D. Mirlin, and D. B. Gutman, Anomalous hydrodynamics in one-dimensional electronic fluid, Phys. Rev. Lett. 126, 256801 (2021)] theories. The kinetic approach is developed by partitioning the Hilbert space into bosonic and fermionic sectors. We focus on the regime where the long-living thermal excitations are fermions and compute thermal conductivity. From the kinetic theory standpoint, the fermionic part of thermal conductivity is normal, while the bosonic one is anomalous, that scales as ω−1/3 and thus dominates in the infrared limit. The multi-mode hydrodynamic theory is obtained by projecting the fermionic kinetic equation on the zero modes of its collision integral. On a bare level, both theories agree and the thermal conductivity computed in hydrodynamic theory matches the result of the kinetic equation. The interaction between hydrodynamic modes leads to renormalization and consequently to anomalous scaling of the transport coefficients. In a four-mode regime, all modes are ballistic and the anomaly manifests itself in Kardar-Parisi-Zhang-like broadening with asymmetric power-law tails. "Heads" and "tails" of the pulses contribute equally to thermal conductivity, leading to ω−1/3 scaling of heat conductivity. In the three-mode regime, the system is in the universality class of a classical viscous fluid [Herbert Spohn, Nonlinear fluctuating hydrodynamics for anharmonic chains, J. Stat. Phys. 154, 1191 (2014); O. Narayan and S. Ramaswamy, Anomalous heat conduction in one-dimensional momentum-conserving systems, Phys. Rev. Lett. 89, 200601 (2002)].

1. INTRODUCTION

The viscous electronic fluids were envisioned in the pioneering work of Gurzhi[1] in the late sixties. Nowadays experiments resurrected the field.[2–24] From the fundamental perspective the interest in electron hydrodynamics stems from its universality, that systems with very different constituents show in the long-range limit. Besides this emergent similarity in the hydrodynamic limit, there are important differences. One special feature of low-dimensional hydrodynamics is a large number of conservation laws.[25,26] For systems that are close to integrable, this number is very large and becomes infinite at the integrability point.[27–31] The combined effects of non-linearity and fluctuations lead to strong renormalization effects[32] manifested in anomalous transport, in particular in thermal conductivity.

For non-interacting electronic systems, there is not much sense to study thermal conductivity, because it is related to the electric one via Wiedemann-Franz law. In the interacting system, this law does not apply and thermal transport reveals information that is not accessible by measuring charge transport. Due to experimental and theoretical challenges, thermal transport is far less explored than charge transport. Recently, the situation has changed, and energy transport was measured in several experiments. The universal value of thermal conductance $g_0 = \pi^2 T/3h$ was observed[33–36] in various devices with ideal point contacts. Heat Coulomb blockade was observed in Ref. 37, directly demonstrating the energy-charge separation in a controllable manner. The propagation of heat in the quantum- Hall-effect regime was studied via quantum-dot[38,39] and shot-noise[40] thermometry.

The experimental progress combined with open fundamental questions prompted us to study thermal transport in a one-dimensional (1D) electronic fluid. The key step in the transition from many-body quantum problem to the classical regime is inelastic scattering between the electrons. For such scattering to occur one has to break the integrability of the problem. For one-dimensional electron without disorder, this requires a finite curvature in the single particle spectrum.[41–45]

The bosonization of electrons with finite spectrum curvature maps non-interacting fermionic theory onto the interacting bosonic one.[46–49] Adding a generic forward scattering interaction between electrons, one thus describes interacting electrons by a non-linear bosonic theory. This bosonic theory can be refermionized,[44,50,51] giving rise to the description of the system in terms of a new fermionic quasiparticles (composite fermions). They are related to the original electrons via non-linear unitary transformation. Bosonic and composite fermion approaches are dual. The curvature in the single-particle spectrum of the bosons corresponds to the interaction of the composite fermions and the other way around. We call this freedom of description the Fermi−Bose duality.[50]

From the mathematical perspective, the duality between fermions and bosons in 1D relies on an exact mapping between the fermionic and bosonic Hilbert spaces.[52,53] The mathematical equivalence of the two languages does not imply that they are equally convenient for performing the computations. In particular, various physical processes are described in these two complementary pictures with varying levels of complexity. One criterion that indicates which type of statistics (Fermi or Bose) is preferential is the longevity of the excitation.[50] By comparing the lifetime of thermal (with energy of the order of temperature) excitation we determine which type of excitations is more natural. Of course, such criteria assume that the dominant excitations are thermal. Moreover, it ignores the fact that different many-body configurations have the same momentum, thus our separation procedure is only an approximation.

Within this approximation, the transition between the fermionic and bosonic regime is determined by the effective mass of fermionic excitations m^* and a length l quantifying the curvature of the bosonic spectrum and the temperature. One can define a temperature scale $T_{FB} = 1/m_* l^2$. At $T < T_{FB}$ the thermal fermions are long-living excitations; the perturbation theory in their interaction is well-behaved and controlled by the small parameter T/T_{FB}. At higher temperatures, $T > T_{FB}$, the proper thermal excitations are bosons and the bosonic perturbation theory possesses a small parameter T_{FB}/T. In this review, we focus on the regime where $T < T_{FB}$, such that the thermal excitations are fermionic. Nevertheless, the existence of a subthermal boson is crucial for thermal conductance in the infrared limit. Below we discuss and compare two different ways of addressing the problem of thermal transport. The first approach[54] is to compute the thermal conductivity by using the kinetic-equation framework within a Bose-Fermi duality picture. The second approach[55] is to start at the Fermi side of the Bose-Fermi duality, then map the problem onto the classical fluctuation hydrodynamics, and finally compute the conductivity within the hydrodynamic formalism by taking into account renormalization effects.

2. HIERARCHY OF SCALES

We now summarise the significant scales of transport regimes. The shortest time scale is determined by three-fermion collisions,[44,45,50,56] for the details of the derivation see Appendix B 2,

$$\frac{1}{\tau_F(k)} = \begin{cases} \dfrac{\gamma l^4 T k^6}{m_*^2 u^2}, & k > \dfrac{T}{u}, \\ \dfrac{\gamma l^4 T^7}{m_*^2 u^8}, & k < \dfrac{T}{u}. \end{cases} \tag{1}$$

Here, γ is a dimensionless parameter that describes the strength of the electron-electron interaction, e.g., Eq. (46). This scattering time corresponds to the spatial scale $L_6 = u\tau_F(T/u)$. For lengths greater than L_6 electrons form a classical fluid. Note that the process of three-fermion-collision involves two fermions from one chiral branch and one fermion from another branch. All fermions involved in the collision typically possess the momentum that is of the order of the thermal momentum ($p_T \simeq T/u$). If two right-moving fermions scatter with the assistance of a left-moving fermion, the change of the momentum for each of the right-moving fermions is of the order T/u. On the other hand, the change in momentum of the left fermion (and thus the momentum exchange between different chiral sectors) $\delta p \simeq T^2/\varepsilon_F u \ll p_T$. Thus, for length scales shorter than

$$L_4 \simeq u\tau_F(p)\left(\frac{p}{\delta p}\right)^2 \simeq \frac{m_*^4 u^{13}}{\gamma l^4 T^9} \tag{2}$$

the energy, momentum, and number of left and right-moving electrons are separately conserved and electrons admit a 6 mode hydrodynamic description. In also useful to define the corresponding frequency scale

$$\omega_4 = \frac{u}{L_4} \simeq \frac{\gamma l^4 T^9}{m_*^4 u^{12}}. \tag{3}$$

This conservation is not exact, and deviations become significant at the scale L_4. At this scale, chiral energies and momenta are no longer separately conserved. Therefore at this scale, these modes reduce the total energy and total momentum. However, left and right particle densities are still well-defined. Therefore the problem is described by 4 mode hydrodynamics. Finally, there is equilibration of the particle numbers between different chiral branches. This process can be visualized as a diffusion of the hole through the bottom of the conduction band. The inter-branch fermion scattering rate[56–59] reads

$$L_U \sim u^2 T^{\ 3/2} \varepsilon_F^{1/2} e^{\frac{\varepsilon_F}{T}}, \tag{4}$$

and a corresponding time $\tau_U = L_U/u$. In addition to the classification based on the conservation laws that we just described, there is a scale that is determined by the renormalization effects. It was shown[55] that renormalization of the bare parameters by fluctuations and non-linearity become significant for lengths greater than $L_* \simeq \frac{u^{13}}{l^{12}T^{13}}$. Thus we arrived at the following hierarchy of scales $L_6 \ll L_4 \ll L_* \ll L_U$. It implies that the renormalization effect occurs deeply in the 4-mode regime. Because physics in 6 mode regime, modus mutandis, is quite similar to the 4 mode regime we will skip from discussing the former. We next describe the heat transport in one-dimensional electronic fluid from the point of view of kinetic theory.

3. HEAT CONDUCTIVITY FROM THE KINETIC EQUATION

In the framework of Bose-Fermi duality, one uses bosonic and fermionic kinetic equations, each one for the corresponding sector of the Hilbert space. The two kinetic equations read

$$\frac{\partial N_\alpha(q)}{\partial t} + u_q^\alpha \frac{\partial N_\alpha(q)}{\partial x} = I_{\alpha,q}[N_\alpha]. \tag{5}$$

Here, $\alpha = F/B$ specifies the type of the quasi-particles (Fermi/Bose), N_α is a distribution function and I_α is the collision integral. In either fermionic or bosonic approach, the energy current can then be computed as

$$J_\alpha(\omega) = \int (dq) u_q^\alpha \omega_q^\alpha N_\alpha(q). \tag{6}$$

Here, the dispersion relation and the Fermi velocity for fermions are given by

$$\omega_q^F = \pm uq + q^2/2m^*, \quad u_q^F = \pm u + q/m^*. \tag{7}$$

Similarly for the bosons

$$\omega_q^B = u_q^B|q|, \quad u_q^B = u\Big((1 - l^2 q^2\Big). \tag{8}$$

In Eq. (7) the ± sign refers to the right and left movers; $(dq) \equiv \frac{dq}{2\pi h}$ and we set $\hbar = 1$ throughout the manuscript.

The total conductivity consists of the ballistic part (that is carried by "almos" zero modes) σ^{bal} and the part that is carried by the excitation with the finite lifetime $\sigma'(\omega)$

$$\sigma(\omega) = \sigma^{\mathrm{bal}}(\omega) + \sigma'(\omega). \tag{9}$$

The finite mode conductivity is carried by two parallel channels (fermionic and bosonic)

$$\sigma'(\omega) = \sigma^F(\omega) + \sigma^B(\omega) \simeq \max\left[\sigma^F(\omega), \sigma^B(\omega)\right]. \tag{10}$$

The contribution of the (almost) zero mode to the heat conductivity can then be extracted either in fermionic or bosonic framework[60,61]

$$\sigma^{\mathrm{bal}}(\omega) = \frac{\pi}{3}\frac{uT}{i\omega + \tau_U^{1}} \simeq \frac{\pi}{3}\frac{uT}{i\omega}. \tag{11}$$

At $\omega\tau_U \gg 1$,

$$\sigma^{\mathrm{bal}}(\omega) = \frac{\pi}{3}\frac{uT}{i\omega} \tag{12}$$

is purely imaginary and does not contribute to the dissipative real part of the total thermal conductance. In the opposite limit, $\omega\tau_U \ll 1$ the contribution of $\sigma^{\mathrm{bal}}(\omega)$ becomes a (large) frequency-independent constant, $\sigma^{bal} = \pi\tau_U uT/3$.

Let us now turn to the analysis of the relaxing modes in the kinetic Eq. (5). Employing the relaxation-time approximation for its solution, we find

$$\mathrm{Re}\sigma^F(\omega) \simeq \frac{T^2}{m_*^2 u^2}\mathrm{Re}\int_0^{T/u} \frac{(dq)}{\tau_F^{1}(q) - i\omega}, \tag{13}$$

for the fermionic and

$$\mathrm{Re}\sigma^B(\omega) \simeq \frac{T^4 l^4}{u^2} \mathrm{Re} \int_0^{T/u} \frac{(dq)}{\tau_B^{\ 1}(q) - i\omega}, \tag{14}$$

for the bosonic representation of the theory, respectively, see Appendix B 3 and A 2. In Eqs. (14) and (13) $\tau_B\ (q)$ and $\tau_F\ (q)$ denote the relaxation times for the bosons and fermions, respectively. Equations (13) and (14) represent contributions of fermionic and bosonic quasiparticles to the thermal conductivity.

We now calculate the real part of thermal conductivity as a function of ω and T, using decay rates Eqs. (A10) and (B12). For $T < T_{FB}$, we find[54]

$$\sigma'(\omega) \sim \begin{cases} \dfrac{T^{\frac{11}{3}} l^4 u^{\ \frac{5}{3}} m_*^{\frac{2}{3}}}{\omega^{\frac{1}{3}}}, & \omega < \dfrac{\gamma^3 T^{23} m_*^2 l^{24}}{2}, \\ \dfrac{u^5}{\gamma T^4 l^4}, & \dfrac{\gamma^3 T^{23} m_*^2 l^{24}}{u^{20}} < \omega < \omega_4. \end{cases} \tag{15}$$

At sufficiently high frequencies, $\omega \gg 1/\tau_U$, the ballistic mode associated with the conservation of the momentum of bosonic excitations do not contribute to the real part of $\sigma(\omega)$ and $\sigma(\omega) \approx \sigma'(\omega)$. At $\tau_U\omega \lesssim 1$ the ballistic channel of the energy propagation becomes gapped and contributes an exponentially large but frequency-independent constant $\sigma^{\mathrm{bal}} \simeq \pi u T \tau_U/3$ to the thermal conductivity.

The computations done in this section were based on the kinetic theory, which includes both Fermi and Bose channels. The latter was studied within the self-consistent scattering approximation. Let us now look at the problem from the hydrodynamic point of view.

4. HEAT CONDUCTIVITY FROM THE HYDRODYNAMIC APPROACH

4.1. Conservation laws and multi-mode hydrodynamics

In the six-mode regime the particle densities, momentum, and energies of each chiral sector are separately conserved and we combine them into two chiral vectors $\mathbf{q}_\eta^T = (\rho_\eta, \pi_\eta, \varepsilon_\eta)$, $\eta = R, L$. We denote by $\phi_\eta^T = T_\eta^{\ 1}(\mu_\eta, \upsilon_\eta, \ -1)$ the vector of the corresponding conjugate variables that are zero modes of the collision integral. The conserved densities obey the set of continuity equations

$$\partial_t q_\eta^i + \partial_x J_\eta^i = 0, \tag{16}$$

with index i specifying the conserved charge and the corresponding flux $J_\eta = (J_\eta^\rho, J_\eta^\pi, J_\eta^\varepsilon)$. On the linear level, one relates

$$q_\eta(\omega, k) = \chi_\eta^{\mathrm{ret}}(\omega, k)\phi_\eta(\omega, k), \tag{17}$$

via the polarization operator

$$\chi_{i,j;\eta}^{\mathrm{ret}}(x, t) = -i\theta(t)\langle[q_{i,\eta}(x, t), q_{i,\eta}(0, 0)]\rangle.$$

Similarly, currents can be represented in terms of current response function M,

$$J_\eta(\omega, k) = M_\eta(\omega, k)\phi_\eta(\omega, k)/ik. \tag{18}$$

In the $\omega = 0$, small-k limit, the matrix $M_\eta(k) = (ikA + k^2 D)\chi_\eta$ is built out of matrices of velocities A, diffusion coefficients D, and static susceptibilities $\chi_\eta \equiv \chi_\eta^{\mathrm{ret}}(\omega = 0, k \to 0)$. All these quantities can be computed directly from the kinetic equation written in terms of the composite fermions Eq. (B5). See Appendix D 2 for the details.

To incorporate non-linear effects into the hydrodynamic description, we extend the expressions for hydrodynamic currents up to second order in the conserved densities:

$$J_\eta = (M_\eta/ik)\chi_\eta^{\ 1} q_\eta + \frac{1}{2}\sum_{i,j} H_{\eta;i,j} q_\eta^i q_\eta^j. \tag{19}$$

Here, we have taken the static limit $\omega = 0$ and the (vectorvalued) coefficients $H_{\eta;i,j}$ can be computed neglecting the interaction of composite fermions, see Appendix D 1.

Equations (16), (17), and (19) describe the six-mode hydrodynamics that exist at scales, $L_6 < L < L_4$. At longer scales, the collisions equilibrate the temperatures and boost velocities in the two chiral sectors. The hydrodynamic theory of the four-mode regime can be obtained through the reduction of the six-modes equations by setting $T_L = T_R = T$, $\upsilon_L = \upsilon_R = \upsilon$, and working with the total energy and momentum densities, $\varepsilon = \varepsilon_R + \varepsilon_L$ and $\pi = \pi_R + \pi_L$.

At still larger length scales, $L > L_U$, the system reaches equilibrium with respect to particle exchange between the chiral sectors. The corresponding three-mode hydrodynamics can be obtained through the reduction of the four-mode theory by setting $\mu_L = \mu_R = \mu$.

4.2 Linear responses in 1D fluid

We now consider the linear response properties of the electronic fluid. Generally speaking, an N-component liquid has $N(N\text{-}1)/2$ independent linear response coefficients, that can be computed via the Kubo formula. To be specific, we focus on thermal conductivity, a quantity that describes the rate of irreversible heat propagation. To compute the thermal conductivity, one needs first to define the heat current. In interacting many-body problems, expressions for heat currents are in general rather complicated and spatially non-local. Luckily, the operator of heat current J_T for fluids is local and can be computed by subtracting an advective contribution from the energy current J_E[62]

$$J_T = J_E - \bar{w} J_\rho, \tag{20}$$

where $\bar{w}$ is the enthalpy of the fluid per one electron and J_ρ the particle current. The Kubo formula for thermal conductivity reads[63]

$$\sigma_T(\omega, k) = \frac{1}{-i\omega T}\left[K_{TT}(\omega, k) - K_{TT}(0, 0)\right], \tag{21}$$

where $K_{TT}(\omega, k) = -i\langle[\hat{J}_T(x, t), \hat{J}_T(0, 0)]\rangle^{ret}(\omega, k)$. The correlation function indicates that one needs to average the expression over the fluctuations. To account for such fluctuation we add the Langevin noise to the hydrodynamic theory, transforming it to fluctuating hydrodynamics. The effective theory can be cast in terms of the Keldysh action (also known in the classical limit as Martin-Siggia-Rose), for the details see Appendix D 1. Since at hydrodynamic scales the system is locally at equilibrium, the fluctuation-dissipation theorem holds. Therefore, at the Gaussian level, the retarded part of the polarization operator χ^{ret} determines the Keldysh components and therefore the entire action. The quadratic terms in the hydrodynamic currents correspond to cubic vertices in the action.

Employing Eq. (21) and using the linearized hydrodynamic theory, see Appendix D 2, we find that in the 4mode regime

$$\sigma_T(\omega, k=0) = -\frac{\pi^2 uT}{3i\omega} + \frac{u^5}{l^4 T^4}. \tag{22}$$

The Drude peak corresponds to the ballistic propagation of heat,[60,61] while the real part of conductivity is due to heat diffusion. This reproduces the results we have previously derived with the kinetic equation approach, for the imaginary [Eq. (12)] and the real [Eq. (15)] parts. The consistency between kinetic and fluctuating hydrodynamic approaches was guaranteed, because we have described the same problem using different languages. Indeed, by disregarding the non-linear part of the hydrodynamic action [Eq. (D6)] we neglected the renormalization processes that we have also ignored in the kinetic equation approach. This is justified only up to scales smaller than L_*.

In the four-mode regime, the propagation of all modes is ballistic, and therefore unaffected by renormalization. Hence the imaginary part of the heat conductivity is given by $\text{Im}\,\sigma_T(\omega) = \pi^2 uT/3\omega$. The real part of the heat conductivity, on the other hand, is renormalized for $L_* < L$. Taking the renormalization of the heat conductivity into account, see Appendix D 5.1 for the details, one finds

$$\text{Re}\sigma_T(\omega)\text{sim}uT^{1/3}\omega^{\ \ 1/3}. \tag{23}$$

Finally, we discuss the three-mode regime. In this case, the heat conductivity is determined solely by the static mode. Therefore, the ballistic contribution is suppressed, giving rise to an exponentially large constant: $i/\omega \mapsto \tau_U$. The real part of the thermal conductivity thus scales as, see Appendix D 5.2 for the details,

$$\text{Re}\sigma_T(\omega) \sim uT\tau_U + \frac{T^{7/3}}{m^2u^3}\omega^{\ \ 1/3}. \tag{24}$$

To derive Eqs. (23) and (24) and to perform classical renormalization group (RG) in the fluid, it is elucidating to connect the problem of thermal conductivity with the problem of pulse propagation. We now elaborate on this and explain the connection between these two problems.

4.3 Pulse propagation in the 1D fluid

Let us consider a generic disturbance created in a confined region of the 1D fluid at a given time, while the rest of the fluid is at thermal equilibrium. One can think of it as a narrow peak of particle and/or energy density that was created by the action of an external force and/or by heating. Due to the collisions for the time scales longer than τ_{F*} a disturbance is projected onto eigenmodes of the collision integral. Because different eigenmodes propagate through the fluid with different velocities a disturbance splits into a finite number of peaks.[64]

To find the eigenmodes one needs to diagonalize the hydrodynamic theory on the Gaussian level, i.e. to diagonalize the velocity matrix A. We pass to a new basis $\mathbf{\Psi} = \text{R}\mathbf{q}$, that consists of different combinations of energy, momentum, and particle densities that on the linear level propagate independently, $RAR^{\ \ 1} = \text{diag}(\upsilon_1, \ldots, \upsilon_N)$. In the 4-mode regime, there are two right and two left propagating modes, shown in Fig. (1), left panel. The degree to which the modes are excited depends on the overlap of the disturbance with Ψ_j.

Because of the mode separation caused by different mode velocities, only the diagonal correlations

$$f_j(x,t) = \langle \Psi_j(x,t)\Psi_j(0,0)\rangle \tag{25}$$

play a role in the long-time limit. To account for the effects of the renormalization in the fluid one can treat the interaction between the modes by solving self-consistent Dyson equations. In the current context, this equation is also known as a mode coupling equation.[64,65] While the agreement between the self-consistent Dyson equation and RG theory that flows into a strong coupling limit is by no means guaranteed, it is known that for the Kardar-Parisi-Zhang (KPZ) problem such an approximation has an excellent agreement with a numerical simulation of an exact solution of KPZ theory. Because our problem is very similar to the KPZ, it is natural to expect this approximation to hold as well. Similar agreement was also observed in dynamical structure factor in Bose gas modeled by Gross-Pitaevskii hydrodynamics.[66] It is worth mentioning that KPZ scaling was theoretically predicted[67–69] and experimentally observed in Heisenberg spin chains.[70–72]

Applied to our problem, the mode-coupling equation reads

$$\left(\partial_t + v_j\partial_x - \tilde{D}_j\partial_x^2\right)f_j(x,t) = \int_{\infty}^{\infty} dy \int_0^t ds \times f_j(x-y, t-s)\partial_y^2 R_j(y,s). \tag{26}$$

Here,

$$R_j(y,s) = \frac{1}{T^5}\sum_{l,m=1}^{N} \lambda_{jlm}^2 f_l(y,s) f_m(y,s), \tag{27}$$

$\tilde{D}_j$ are diagonal elements of the effective diffusion matrix $\bar{D}$ describing broadening of eigenmodes, and coupling constants λ_{jlm} account for the mode interaction. These constants are computed from microscopic parameters of the original fermionic model.[55]

We now employ this theory to study pulse propagation in an electronic fluid and reinterpret the shape of the pulses as a renormalization of the corresponding transport coefficients. The spatial separation between the peaks grows linearly with time $L_{ij} = \Delta u_{ij} t$, where the relative velocity $\Delta u_{ij} \equiv u_i - u_j$. The width of each peak is broadened, within the linear hydrodynamics, by the corresponding diffusion process as $(\tilde{D}_j t)^{1/2}$. This is in line with a usual relation between the diffusive broadening of the peak and the diffusion coefficient that is independent of the system length.

The non-linear couplings further broaden the shape of the pulses and modify their shape. Comparing the linear and non-linear terms, one can show that non-linear broadening dominates over the normal diffusion at scales beyond $L_*{=}u^{13}/l^{12}T^{13} \gg L_4$. Therefore, when fluid enters the four-mode regime, it is still governed by essentially linear theory, with conventional diffusive scaling. Therefore, the evolution in earlier stages of the four-mode regime is well approximated by the linearized hydrodynamic theory. But for $L > L_*$ the non-linear terms start to dominate and the normal diffusion process is replaced by the anomalous one. Essentially, at this stage, one can drop the bare diffusion terms in Eq. (26). In the four-mode regime, all non-linear coupling constants are of the same order, $\lambda_{ijk} \sim \lambda \equiv Tu^{3/2}$. However, only the interaction between modes propagating in the same direction is significant. Therefore, Eq. (26) splits into two sets of chiral equations. Near the maximum of any given mode, the coupling to other modes is exponentially small and can be neglected. Note that Eq. (26) in this limit is mathematically equivalent to the mode coupling equation for velocity correlation function in stochastic Burgers equation and corresponding KPZ problem.[73] Therefore near the maximum the pulse is described by the same solution

$$f_i(x,t) \sim \frac{T^2}{(\lambda t)^{2/3}} f_{KPZ}\left(\frac{T(x-u_i t)}{(\lambda t)^{2/3}}\right). \tag{28}$$

Here, $f_{KPZ}\ (x)$ is the universal dimensionless KPZ function, with $f_{KPZ}\ (x) \sim 1$ for $|x| \leq 1$ and $f_{KPZ}(x) \sim e^{\ 0.3|x|^3}$ for $|x| \gg 1$ [74,75] Away from the maximum the interaction between modes plays a role and builds non-symmetric power-law tails Appendix D 4.1, Eq. (D54), see also Fig. 1. The fast-moving mode interacts with the slow-moving mode and thus grows power-law rear tails. The slow mode interacts with the fast-moving mode in front of it and the oppositely moving slow mode, thus growing power-law front and rear tails

$$f_i(x,t) \sim \sum_{j=1}^{3} \theta[(x-u_i t)\mathrm{sgn}(\Delta u_{ji})]u^2\left(\frac{T}{|\Delta u_{ji}|}\right)^{1/3}$$
$$\times\ t|x-u_i t|^{\ 8/3} \text{for } |x-u_i t| \gg \frac{ut^{2/3}}{T^{1/3}}. \tag{29}$$

In Eqs. (28) and (29) and below we omit numerical coefficients of order unity, as emphasized by the sign $\sim$ replacing the equality sign.

At distances larger than L_U, the fluid is described by three hydrodynamic modes. This is a universal regime representing the infrared fixed point of any non-integrable one-dimensional model. It is characterized by two ballistically propagating sound modes (index $j = 2, 3$) and one static heat mode ($j = 1$). The pulse propagation in such a regime was studied in the context of classical fluids in Refs. 64, 65, 76, and 77. The fate of the ballistic sound mode in the 3-mode regime is very similar to the one we just discussed for the 4-mode regime. Due to the self-interaction, the sound modes acquire the KPZ shape, Eq. (28) with a power law rear tail, Appendix D 4.2, Eq. (D57). The value of the self-coupling constant for the sound modes in our model can be estimated as $\lambda \equiv \lambda_{222} \sim T^4/m^3u^{9/2}$.

The evolution of the static mode is qualitatively different. The time-reversal symmetry forbids the self-coupling of the heat mode. The non-linear interaction between the heat and sound mode, which is characterized by a coupling $\lambda_{222} \sim T^3/m^2u^{5/2}$, leads to the formation of power-law tails for the heat and sound modes, see Appendix D 4.2. It transforms the heat mode into symmetric Levy flight distribution with $\alpha = 5/3$,

$$f_1(x,t) \sim \frac{T}{\delta x(t)} f_{\text{Levy},\alpha=5/3}\left(\frac{x}{\delta x(t)}\right). \tag{30}$$

The heat mode has a maximum at $x = 0$ and the width $\delta x(t) \sim t^{3/5}T^{4/5}m^{\ 6/5}u^{\ 7/5}$. The $t^{3/5}$ scaling of the width was also obtained in the context of classical anharmonic chains.[78,79] The value at the maximum is $f_1(0,t) \sim T/\delta x$. Away from the maximum (for $x \gg \delta x$) the heat mode has power law tails[80] that scale [see Appendix D 4.2, Eq. (D56)] as $f_1(x,t) = \frac{T^{7/3}}{m^2u^{7/3}} tx^{\ 8/3}$, implying anomalous heat diffusion.

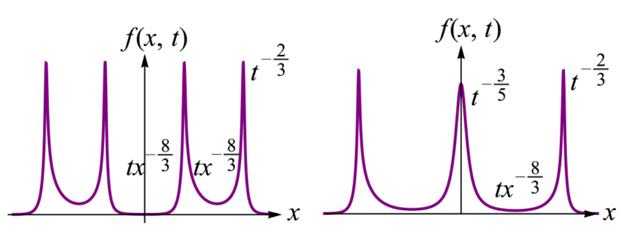

FIG. 1. Schematic shape of pulse evolution through four and three mode regimes. The scaling of the "heads" and "tails" of the peaks with time is depicted, see text for details. From Ref. 55.

5. SUMMARY

We studied thermal transport in one-dimensional electronic fluid combining kinetic and hydrodynamic theories. The kinetic analysis was based on the Fermi-Bose duality picture that enables us to describe the problem in terms of both (fermionic and bosonic) degrees of freedom. To be specific, we focused on the temperature below the Bose-Fermi duality transition temperature ($T < T_{FB}$). In this limit, the thermal fermionic excitations are well-resolved quasi-particles, as opposed to the thermal bosonic excitation.

We derived the viscous multi-mode hydrodynamic theory, by projecting the fermionic kinetic equation on the eigenmodes of its collision integral. Depending on the length scale it may have six, four, and three modes. On a bare level, the kinetic and hydrodynamic theories yield same results for thermal conductivity.

We use the fluctuating hydrodynamic approach to compute the effects of renormalization that arise due to fluctuations combined with non-linearity. This renormalization leads to anomalous heat transport that diverges with the system size. To study the effects of the renormalization we consider a problem of pulse evolution that enables us to effectively compute all transport coefficients. We solve the pulse evolution problem by applying the self-consistent mode coupling approximation. In the six and four-mode regimes, the pulses propagate ballistically. The "head" of every pulse is controlled by self-interaction and has a KPZ scaling with time. The width of the pulse growths as $t^{2/3}$ and its amplitude decreases as $t^{-2/3}$. Interaction between the modes propagating with different velocities results in power-law tails scaling as $x^{-8/3}$ with distance x from the center of the first mode and directed towards the second mode. Therefore the faster-moving modes grow the rear tails, while slower-moving modes grow both the front and rear tails.

In a three-mode regime, there are one static heat and two ballistic sound peaks. The width of the ballistic modes has KPZ scaling with time. The interaction between the sound waves and the heat mode gives rise to power-law tails for all peaks. Each sound mode acquires a rear tail. The static heat mode is a Levy flight function with $\alpha = 5/3$, with symmetric tails. The anomaly in peak shapes leads to anomalous kinetic coefficients, in particular, thermal conductivity.

As expected, the results computed within the kinetic and hydrodynamic theories agree for scales smaller than L_*, where renormalization effects became important. At this scale, the prediction of a bare kinetic theory deviates from the RG analysis we performed within the hydrodynamic framework. However in the infrared limit thermal conductivity computed within the kinetic equation approach is determined by subthermal bosons, even for $T < T_{FB}$ case. Therefore the kinetic approach that contains self-consistent boson scattering yields thermal conductivity with correct $\omega^{-1/3}$ scaling, see, e.g, Eqs. (23) and (24). Such agreement in scaling resulting from self-consistent kinetic[32,81,82] and classical renormalization-group[83] approaches has been known for a long time, but is not fully understood up to this point. By performing $d = 1 + \varepsilon$ expansion one can show that this agreement holds beyond the $d = 1$ case, and thus is not a mere coincidence of numbers. One therefore needs to explain, why this agreement exists in the first place and, at the same time, why it only holds for the scaling and does not reproduce the prefactors.

We now propose a plausible explanation for this puzzle. At the scale L_4 where we constructed the hydrodynamic theory, typical excitations that matter for the thermal transport is indeed thermal, and therefore the problem is equally well accounted for by the fermionic kinetic equation and the hydrodynamic model derived from it. In the infrared limit, this is no longer true and sub-thermal bosons dominate the heat conductivity. From the hydrodynamic perspective, the collective hydrodynamic modes strongly interact. In both theories, the interaction of low bosonic modes is described by three boson vertices and results in the same scaling. It is therefore plausible that both pictures describe the same process, seen from two different viewpoints. What is seen as an effect of renormalization in the classical fluid represents a self-consistent scattering in terms of the bosons. Therefore the agreement of the results is another manifestation of the Fermi-Bose duality. The disagreement regarding the prefactors is probably limited by the accuracy of our procedure. It remains to be seen if a more accurate partition of the Hilbert space can lead to a full agreement.

ACKNOWLEDGMENTS

D. G. was supported by ISF-China 3119/19 and ISF 1355/20.

APPENDIX A: KINETIC THEORY FOR BOSONS

1. Bosonization

In this section, we briefly recap the bosonization approach for electrons with a finite curvature.[50,52,53,84,85] The system of interacting electrons in one dimension is described by the microscopic Hamiltonian

$$H = \sum_{\eta=R/L} \int dx \psi^+_\eta(x) \left(-i\eta \upsilon_F \partial_x - \frac{1}{2m}\partial_x^2 \right) \psi_\eta(x) + \frac{1}{2}\int dx dx' g(x-x')\rho(x)\rho(x'). \tag{A1}$$

After the bosonization procedure, the Hamiltonian can be represented in terms of the density field

$$H = \sum_\eta \int dx \colon \left(\pi \upsilon_F \rho_\eta^2(x) + \frac{2\pi^2}{3m}\rho_\eta^3(x) \right) \colon_B + \frac{1}{2}\int dx dx' g(x-x') \colon \rho(x)\rho(x') \colon_B. \tag{A2}$$

Here, $::_B$ stands for normal ordering with respect to the bosonic modes. The coupling between left and right chiral sectors can be eliminated up to a cubic level by performing unitary transformations, $R = U\rho_R U^+$, $L = U\rho_L U^+$, see Ref. 50 for the details.

After the rotation, the bosonic Hamiltonian reads

$$H = \colon \frac{\pi}{L}\sum_q u_q R_q R_{\ q} + \frac{1}{L^2}\sum_q \Gamma_q^{B,RRR} R_{q_1} R_{q_2} R_{q_3} + \frac{1}{L^3}\sum_q \Gamma_q^{B,RRRL} R_{q_1} R_{q_2} R_{q_3} L_{q_4} \colon_B + (R \leftrightarrow L). \tag{A3}$$

The bosonic vertices Γ_q in Eq. (33) in the low momentum limit ($ql \ll 1$) are

$$\Gamma_q^{B,RRR} = \frac{2\pi^2}{3m_*}\left(1 - \frac{\alpha l^2}{2}(q_1^2 + q_2^2 + q_3^2)\right),$$
$$\Gamma_q^{B,RRR} = \frac{2\pi^2\alpha}{3m_*^2 u}\left(1 - \frac{3\alpha}{2} + \frac{15}{4} l^2 \frac{q_1 q_2 q_3}{q_4}\right). \tag{A4}$$

Here, $m_* = \frac{4\sqrt{K_0}}{3+K_0^2} m$ is renormalised mass of the electron, $\alpha = \frac{1}{3+K_0^2}\frac{K_0^2}{}$ is dimensionless interaction strength, and K_0 is LL parameter. One can define another dimensionless parameter that quantifies the strength of electron interaction

$$\gamma = \alpha^2(1+\alpha)^2. \tag{A5}$$

Next, we employ the Hamiltonian (A2) to derive a kinetic equation for the bosonic distribution function.

2. Kinetic equation

The Fourier components of the densities $R(x)$ and $L(x)$ can be identified with bosonic creation and annihilation operators via

$$R_q = \sqrt{\frac{L\backslash q\backslash}{2\pi}}\left(\Theta(q)b_q + \Theta(-q){b^+}_q\right),$$
$$L_q = \sqrt{\frac{L\backslash q\backslash}{2\pi}}\left(\Theta(q)b_q + \Theta(q){b^+}_q\right). \tag{A6}$$

The bosonic distribution $N_B(q, x, t)$ is defined as

$$N_B(q, x, t) = \frac{1}{2\pi}\int_{\infty}^{\infty} d(q_1 - q_2)e^{i(q_1\ \ q_2)x}\langle b^+_{q_1}(t)b^+_{q_2}(t)\rangle, \tag{A7}$$

where $q = (q_1 + q_2)/2$ and the operators b_q and b^+_q are defined in Eq. (A6). Using a standard Keldysh formalism[86,87] one derives the kinetic equation for bosons

$$\frac{\partial N_q}{\partial t} + u_q\frac{\partial N_q}{\partial x} = I[N_q]. \tag{A8}$$

There are various scattering processes that involve bosons. On the level of the usual golden rule there is a scattering of one boson mode into three. This involves three bosons of the same chirality (e.g., right) and one boson of the opposite chirality.[50,88] Because we focus on the regime $T < T_{FB}$ this processes play no role. We therefore focus on a subtle process controlled by three boson interaction. These processes are described by the vertices $\Gamma_q^{B,RRR}$ and $\Gamma_q^{B,LLL}$, Eq. (A4). The inclusion of this term into self-consistent scattering leads to the following collision integral:

$$I[N_q] = \frac{128\pi}{9m^2}\int_0^q (dp)\frac{pq(q-p)}{\gamma_p + \gamma_{q\ \ p}} \times \left[N_pN_{q\ \ p} - N_q - N_qN_p - N_qN_{q\ \ p}\right]$$
$$+\frac{256\pi}{9m^2}\int_q^{q_{\rm thr}} \frac{pq(q-p)}{\gamma_p + \gamma_{q\ \ p}}\left[N_P + N_pN_q - N_qN_{p\ \ q} + N_pN_{p\ \ q}\right], \tag{A9}$$

Here, the self-consistent Bose decay rate

$$\gamma_q \simeq \frac{1}{\tau_B(q)} = \begin{cases} q^{3/2}\dfrac{\sqrt{T/u}}{m}, & q < q_{\rm thr}, \\ 0, & q > q_{\rm thr} \end{cases} \tag{A10}$$

is rate of a self-consistent boson decay.[32,82] The value of the threshold momentum $q_{\rm thr} = \frac{T^{1/3}}{um^{2/3}l^{4/3}}$ is determined by the condition that the energy level broadening (A10) exceeds the nonlinear correction ul^2q^3 to the bosonic dispersion relation at momentum q. This reproduces the result found in Refs. 32, 81, and 82.

The linearization of this integral yields

$$I = \frac{32}{9m^2}\int_0^q dp\frac{pq(q-p)}{\gamma_p + \gamma_{q\ \ p}}\left[N_p\left(\coth\frac{u(q-p)}{2T} - \coth\frac{uq}{2T}\right)\right.$$
$$-N_q\left(\coth\frac{up}{2T} + \coth\frac{u(q-p)}{2T}\right) + N_{q\ \ p}\left.\left(\coth\frac{up}{2T} - \coth\frac{uq}{2T}\right)\right]$$
$$+\frac{64}{9m^2}\int_q^{q_{\rm thr}} dp\frac{pq(p-q)}{\gamma_p + \gamma_{p\ \ q}}\left[N_p\left(\coth\frac{u(p-q)}{2T} - \coth\frac{uq}{2T}\right)\right.$$
$$+N_{p\ \ q}\left(\coth\frac{up}{2T} - \coth\frac{uq}{2T}\right) + N_q\left.\left(\coth\frac{up}{2T} - \coth\frac{u(p-q)}{2T}\right)\right].$$

For the subthermal bosons ($q \ll q_T$) one can simplify it further

$$I[N_q] \simeq \frac{64}{3m}\sqrt{T/u}\left[-q^{3/2}N_q + \frac{q}{2}\int_q^{q_{\rm thr}} qpp^{\ \ 1/2}N_p\right]. \tag{A11}$$

Now we turn to the computation of the thermal conductivity. The real part of thermal conductivity carried by the bosonic excitations in the low-frequency regime is controlled by self-consistent Boson scattering[55]

$$\mathrm{Re}\ \sigma^B(\omega) \simeq \frac{T^4l^4}{u^2}\mathrm{Re}\left[\int_0^{T/u}\frac{(dq)}{\tau_B^{\ 1}(q) - i\omega}\right]. \tag{A12}$$

The momentum integration in Eq. (42) is cut by the value of the thermal momentum T/u, because beyond it, the integrand is exponentially suppressed. By comparing the self-consistent one-into-two boson decay rate with the one-into-three boson decay rate one observes that the first one is faster, for $q < q_{\rm thr}$, i.e. in the regime we are interested in the current paper. Thus, the bosonic contribution to the thermal conductivity is given by

$$\mathrm{Re}\sigma^B(\omega) = \frac{T^{\frac{11}{3}}l^4u^{\ \frac{5}{3}}m_*^{\frac{2}{3}}}{\omega^{\frac{1}{3}}}, \quad \omega < \frac{T^2}{m_*u^2}. \tag{A13}$$

APPENDIX B: KINETIC THEORY FOR FERMIONS

1. Refermionization

The bosonized Hamiltonian (A3) can be recast in terms of fermionic operators as

$$R_q = \sum_k c^\dagger_{R,k}c_{R,k+q}, \quad L_q = \sum_k c^\dagger_{L,k}c_{L,k+q}. \tag{B1}$$

This results in a refermionised Hamiltonian[89]

$$H=\sum_k \varepsilon_{R,k}{:}c^\dagger_{R,k}c_{R,k}{:}_F+\frac{1}{L}\sum_k \Gamma_k^{F,RR}{:}c^\dagger_{R,k_1}c^\dagger_{R,k_2}c_{R,k_2'}c_{R,k_1'}{:}_F$$
$$+\frac{1}{L}\sum_k \Gamma_k^{F,RL}{:}c^\dagger_{R,k_1}c^\dagger_{L,k_2}c_{L,k_2'}c_{R,k_1'}{:}_F$$
$$+\frac{1}{L^2}\sum_k \Gamma_k^{F,RRR}{:}c^\dagger_{R,k_1}c^\dagger_{R,k_2}c^\dagger_{R,k_3}c_{R,k_3'}c_{R,k_2'}c_{R,k_1'}{:}_F$$
$$+\frac{1}{L^2}\sum_k \Gamma_k^{F,RRL}{:}c^\dagger_{R,k_1}c^\dagger_{R,k_2}c^\dagger_{L,k_3}c_{L,k_3'}c_{R,k_2'}c_{R,k_1'}{:}_F+(R\leftrightarrow L). \quad \text{(B2)}$$

We denote by k in each of vertices $\Gamma_k^{F,\cdots}$ the full set of all momenta of the fermionic operators involved. As shown in Ref. 50 the dominant vertex for energy relaxation is $\Gamma_k^{F,RRL}$. In the bosonic description, it corresponds to 1 boson going into 3 bosons scattering process, e.g. Equation (A4).

$$\Gamma_k^{F,RRL}=\frac{5\alpha l^2\pi^2(k_1-k_2)(k_1'-k_2')}{16m^{*2}u(k_3-k_3')}\times\left[(k_1-k_2)^2-(k_1'-k_2')^2\right]. \quad \text{(B3)}$$

2. Kinetic Equation

Using the Keldysh formalism, one can derive a kinetic equation for the fermionic distribution $N_k(x,t)$

$$N(k,x,t)=\int_{-\infty}^{\infty}\frac{d(k_1-k_2)}{2\pi}e^{i(k_1-k_2)x}\langle c^+_{k_1}(t)c_{k_2}(t)\rangle, \quad \text{(B4)}$$

where $k=\frac{k_1+k_2}{2}$ and the operators c_k andc_k^+ are defined in Eq. (45). By repeating the standard steps of Keldysh formalism with the Hamiltonian (45) one derives the kinetic equation for composite fermions

$$\frac{\partial N_k}{\partial t}+\upsilon_k\frac{\partial N_k}{\partial x}=I[N_k]. \quad \text{(B5)}$$

Here, $\upsilon_k=\partial_k\varepsilon_k$ is a velocity of fermions, $\varepsilon_k=\frac{k^2}{2m_*}-\frac{k_F^2}{2m_*}$, and $k_F=m^*u$. The fermionic collision integral I[N] is given by

$$I[N]=I_{\rm out}[N]+I_{\rm in}[N]. \quad \text{(B6)}$$

Here,

$$I_{\rm out}[N]_k=-\sum_{k_2,k_3,k',k_2',k_3'}W_{kk_2k_3}^{k',k_2',k_3'}N_kN_{k_2}N_{k_3}(1-N_k)(1-N_{k_2'})(1-N_{k_3'})$$

is outgoing

$$I_{\rm in}[N]_k=\sum_{k_2,k_3,k',k_2',k_3'}W_{kk_2k_3}^{k',k_2',k_3'}(1-N_k)(1-N_{k_2})(1-N_{k_3})N_kN_{k_2'}N_{k_3'}$$

and incoming parts. The matrix element of three fermion collision[50] is given by

$$W_{kk_2k_3}^{k',k_2',k_3'}=\frac{\gamma l^4}{m_*^2u}(k_2-k)^2(k_2'\text{-}k')^2\delta(k_2+k-k_2'-k')\delta(k_3-k_3').$$

Near the equilibrium, one can linearize the collision integral using the ansatz

$$N=n+gf. \quad \text{(B7)}$$

Here, n denotes the local equilibrium Fermi-Dirac distribution $n_k=\frac{1}{e^{\varepsilon_k/T}+1}$ and $g_k=\sqrt{n_k(1-n_k)}=\frac{1}{2\cosh\varepsilon_k/2T}$

After Fourier transforming it in time, the linearized Boltzmann equation reads

$$-i\omega f_k+B_k^F\frac{\nabla T}{T^2}=\mathcal{J}[f]_k, \quad \text{(B8)}$$

where

$$B_k^F=\upsilon_k\varepsilon_kg_k. \quad \text{(B9)}$$

and the linearized collision integral $\mathcal{J}$ is

$$\mathcal{J}[f]_k=\frac{\gamma Tl^4}{m_*^2u^2}\times\int_{-\infty}^{\infty}dk_2\int_{-\infty}^{\infty}dk'\int_{-\infty}^{\infty}dk_2'(k-k_2)^2(k'-k_2')^2\delta(k+k_2-k'-k_2')$$
$$\times g(k_2)g(k')g(k_2')\left(\frac{f(k)}{g(k)}+\frac{f(k_2)}{g(k_2)}-\frac{f(k')}{g(k')}-\frac{f(k_2')}{g(k_2')}\right). \quad \text{(B10)}$$

On the level of diagonal approximation, we find the decay rate

$$\tau_F^{-1}(k)=\frac{\gamma Tl^4}{g(k)m_*^2u^2}\int_{-\infty}^{\infty}dk_2\int_{-\infty}^{\infty}dk'\int_{-\infty}^{\infty}dk_2'(k-k_2)^2(k'-k_2')^2$$
$$\times\delta(k+k_2-k'-k_2')g(k_2)g(k')g(k_2'). \quad \text{(B11)}$$

This yields a fermionic lifetime

$$\frac{1}{\tau_F(q)} = \begin{cases} \dfrac{\gamma l^4 T k^6}{m_*^2 u^2}, & k > \dfrac{T}{u}, \\ \dfrac{\gamma l^4 T^7}{m_*^2 u^8}, & k < \dfrac{T}{u} \end{cases} \tag{B12}$$

reproducing the results of Refs. 44, 45, 50, and 56.

3. Thermal conductivity via kinetic equation

Next, we compute the thermal conductivity in the fermionic channel. Since fermions are massive particles, one should impose a zero momentum transfer condition.[90] It is achieved by subjecting the system to the gradient of the chemical potential $\Delta\mu$. After this procedure, we are left with B^F that is a part of B^F orthogonal to the *momentum* zero mode$\phi_p = \frac{1}{\sqrt{2m_* T k_F}} k g_k$.

In the orthogonal subspace, we now further decompose it into parts parallel and perpendicular to the number zero mode $\phi_n = \sqrt{\frac{k_F}{2m_* T}}\mathrm{sgn}(k) g_k$. This results in the decomposition $\mathcal{B}^F = \mathcal{B}^F_{\parallel} + \mathcal{B}^F_{\perp}$. To leading order in T,

$$\begin{aligned} \mathcal{B}^F_{\parallel} &= \frac{\sqrt{2} k_F^{\frac{5}{2}} T^{\frac{1}{2}}}{m_*^{\frac{3}{2}}} (\phi_p - \phi_n), \\ \mathcal{B}^F_{\perp} &= \mathcal{B}^F - \frac{\sqrt{2m_*}\pi^2 T^{\frac{5}{2}}}{3 k_F^{\frac{3}{2}}} \phi_p - \mathcal{B}^F_{\parallel}. \end{aligned} \tag{B13}$$

We now substitute this decomposition into Eq. (B8) and compute the thermal conductivity. Within the diagonal approximation, one can solve the Boltzmann equation Eq. (B8)

$$f_{\mathrm{bal}} = \frac{\mathcal{B}^F_{\parallel}}{-i\omega} \frac{\nabla T}{T^2}, \quad f_{\perp} = \frac{\nabla T}{T^2} \frac{\mathcal{B}^F_{\perp}}{\tau_F^{\ 1} - i\omega}. \tag{B14}$$

Thus, the ballistic part of the thermal current is given by

$$J_{\mathrm{bal}} = \frac{\pi}{3} \frac{Tu}{i\omega} \nabla T.$$

The ballistic part of the thermal current matches the one found within the bosonic approach. This happens because in both descriptions it is fully controlled by a corresponding (bosonic and fermionic) momentum zero modes.

The real part of thermal conductivity is thus given by

$$\mathrm{Re}\sigma^F(\omega) \simeq \frac{T^2}{m_*^2 u^2} \mathrm{Re} \int_0^{\frac{T}{u}} \frac{(dq)}{\tau_F(q)^{\ 1} - i\omega}. \tag{B15}$$

Employing Eq. (B12) for the fermionic lifetime, one finds

$$\mathrm{Re}\sigma^F(\omega) = \frac{u^5}{\gamma T^4 l^4}, \quad \omega < \omega_4. \tag{B16}$$

APPENDIX C: TOTAL THERMAL CONDUCTIVITY VIA THE KINETIC EQUATION: BOSONS AND FERMIONS

As we showed above, there are two channels of energy transport in 1D electronic fluid: fermionic and bosonic. The resulting contribution to thermal conductivity is given by a sum of bosonic and fermionic parts. For the imaginary part of the thermal conductivity, both fermionic and bosonic channels yield identical results, and therefore one may use either description. For the real part of the thermal conductivity, this is not the case. However, since $\mathrm{Re}\,\sigma \sim \tau$, it is automatically determined by the long-living species. Therefore, up to a numerical prefactor, the result can be obtained by summing both contributions.

In the high-frequency limit, fermions dominate the thermal conductivity. Below a critical frequency, $\omega_* = \gamma^3 T^{23} m_*^2 l^{24} u^{\ 20}$ bosons dominate it. At the crossover frequency $\tau_B\ (\omega_*) > \tau_F\ (\omega_*)$, which implies that the bosons are good quasi-particles and the dominant contribution was found correctly. The inequality remains true even at lower frequencies as the bosonic excitations become more long-lived at low frequencies while the fermionic lifetime remains constant. The result is

$$\mathrm{Re}\sigma'(\omega) = \begin{cases} \dfrac{T^{\frac{11}{3}} l^4 u^{\ \frac{5}{3}} m_*^{\frac{2}{3}}}{\omega^{\frac{1}{3}}}, & \omega < \dfrac{\gamma^3 T^{23} m_*^2 l^{24}}{u^{20}} \\ \dfrac{u^5}{\gamma T^4 l^4}, & \dfrac{\gamma^3 T^{23} m_*^2 l^{24}}{u^{20}} < \omega < \omega_4. \end{cases} \tag{C1}$$

APPENDIX D: FLUCTUATING HYDRODYNAMICS

1. Action

In this section, we formulate the Martin-Siggian-Rose action for fluctuating hydrodynamics. Our goal is to derive an effective action such that the correlation functions are computed as

$$\langle\rangle = \int \mathcal{D}q\mathcal{D}\bar{q} e^{iS[q,q]}. \tag{D1}$$

We start with the Gaussian part of the action

$$S_0 = \left(\mathbf{q}^T, \mathbf{q}^T\right)_{\omega,\ \ k} T \widehat{\chi}_{\omega,k}^{\ 1} \begin{pmatrix} \mathbf{q} \\ \mathbf{q} \end{pmatrix}_{\omega,k}, \tag{D2}$$

here, we denote

$$\widehat{\chi}_{\omega,k}^{\ 1} = \begin{pmatrix} 0 & \widehat{\chi}_{\omega,k}^{\mathrm{a}\ 1} \\ \widehat{\chi}_{\omega,k}^{\mathrm{r}\ 1} & \left(\widehat{\chi}_{\omega,k}^{\mathrm{r}\ 1} - \widehat{\chi}_{\omega,k}^{\mathrm{a}\ 1}\right) B_{\omega} \end{pmatrix}, \tag{D3}$$

where $B_\omega = \coth\left(\frac{\omega}{2T}\right)$. The action is encoded by

$$\chi_\eta^{\ 1}(\omega, k) = i\omega M_\eta^{\ 1}|(k) + \chi_{0,\eta}^{\ 1}(k). \tag{D4}$$

In the limit ω→0 the expansion

$$M_\eta(k)\chi_{0,\eta}^{\ 1}(k) = ikA_\eta + k^2 D_\eta. \tag{D5}$$

Yield the generalized velocity A and diffusion D matrices. Their size is equal to the number of conserved modes. Because the system is in local equilibrium, analytic properties, and fluctuation-dissipation theorem allow to restore advance and Keldysh components, $\chi^K(\omega, k) = [\chi^{\rm ret}(\omega, k) - \chi^{\rm adv}(\omega, k)]\coth\frac{\omega}{2T}$. The term in the action involving the Keldysh component χ describes thermal fluctuations.

The interaction part of the action

$$S_{\rm int} = -iT\sum_{p,l,m} \bar{q}^p \Gamma_{p,l,m} q^l q^m, \tag{D6}$$

and the interaction vertex

$$\Gamma_{p,l,m}(k) = k\sum_{p1} M_{-p,p_1}^{\ \ 1}(k) H_{l,m}^{p_1}(k). \tag{D7}$$

Here,

$$H_{l,m}^p(k) = \frac{\partial^2 J_p(k)}{\partial q_1 \partial q_m}. \tag{D8}$$

Because matrices M and χ are symmetric, the Keldysh action (D2) can be diagonalized as a quadratic form by the linear transformation

$$\mathbf{q} = R^{\ 1}\boldsymbol{\Psi}, \quad \bar{\mathbf{q}} = R^{\ 1}\boldsymbol{\Psi}. \tag{D9}$$

Since the compressibility matrix has positive eigenvalues, one can choose

$$\frac{1}{T}R\chi_0 R^T = \hat{1} \tag{D10}$$

and

$$RAR^{\ 1} = \hat{\upsilon}. \tag{D11}$$

Here, $\hat{\upsilon} = {\rm diag}\ (\upsilon_1, \upsilon_{2,} \ldots)$ is the diagonal velocity matrix. This implies an identity

$$\frac{1}{T}RMR^T = ik\hat{\upsilon} + \tilde{D}k^2, \tag{D12}$$

Where $\tilde{D} = RDR^{\ 1}$ is the diffusuion matrix in the eigen-mode basis. After the rotation (D9), the retarded part of the Gaussian action takes the form

$$S_0^{\rm ret}[\Psi] = \sum_{m,n} \Psi_m^T(-\omega, -k)\left[i\omega(i\hat{\upsilon}k + k^2\tilde{D})^{\ 1} + \hat{1}\right]_{m,n} \Psi_n(\omega, k). \tag{D13}$$

The corresponding retarded propagator reads

$$G^r(\omega,\ k) = i\langle\Psi_m\Psi_n\rangle_{\omega,k} = \left(i\omega\left(i\hat{\upsilon}k - \tilde{D}k^2\right)^{\ 1} + 1\right)_{m,n}^{\ 1}. \tag{D14}$$

The advanced propagator is related to the retarded one via

$$G^a(\omega, k) = i\langle\Psi_m\Psi_n\rangle_{\omega,k} = -i\langle\Psi_m\Psi_n\rangle_{\omega,k}^*. \tag{D15}$$

The Keldysh part of the propagator f1ollows from FDT theorem[90]

$$\begin{aligned} f(\omega, k) &\equiv \langle\Psi_m\Psi_n\rangle(\omega, k) \\ &= [\langle\Psi_m\Psi_n\rangle(\omega, k) - \langle\Psi_m\Psi_n\rangle(\omega, k)]_{m,n}\coth\frac{\omega}{2T}. \end{aligned} \tag{D16}$$

In the coordinate-time representation (D14) and (D16) read

$$G^r(x, t) = -i\theta(t)\partial_t \frac{\exp\left(-\dfrac{(x+\upsilon t)^2}{4Dt}\right)}{\sqrt{Dt}}. \tag{D17}$$

Using the classical limit of FDT ($T \gg \omega$)

$$f(\omega, k) \simeq \left[G^r(\omega, k) - G^a(\omega, k)\right]\frac{2T}{i\omega} \tag{D18}$$

one finds

$$f(x, t) = T\frac{\exp\left(-\dfrac{(x+\upsilon t)^2}{4D|t|}\right)}{\sqrt{D|t|}}. \tag{D19}$$

From here one infers an equal time correlation function in x −1 representation $f(x,0) = T\delta(x)$.

Next, we discuss the non-linear part of the action. In terms of eigenmodes Ψ

$$\begin{aligned} S_{\rm int} &= \sum_{k,l,m}\int dx_1 dx_2 \gamma_{k,l,m}(x_1 - x_2)\bar{\Psi}_k^T(x_1)\Psi_l(x_2)\Psi_m(x_2) \\ &= \sum_{k,l,m}\ \sum_{p,p_1}\gamma_{k,l,m}(p)\bar{\Psi}_k^T(p)\Psi_l(p_1 - p)\Psi_m(-p_1). \end{aligned} \tag{D20}$$

Here, the vertex of the interaction

$$\gamma_{k,l,m}(p) = T\sum_{k_1,l_1,m_1} R_{k,k_1}^{\ 1^T}\Gamma_{k_1,l_1,m_1}(p)R_{l_1,l}^{\ 1}R_{m_1,m}^{\ 1}. \tag{D21}$$

and we denote $f_n(x, t) = \langle\Psi_n(x, t)\Psi_j(0, 0)\rangle$ for $n = j$.

In this part of SM, we derive the response coefficients that appear in Eqs. (7) and (8) of the main text for the 4- and 3-mode regimes. To keep the presentation concise we skip the discussion of the six-mode regime. For details of the 6-mode regime see Refs. 55 and 91. We also construct the eigenmodes Ψ of linearised hydrodynamics in all the regimes, defined in the main text, compute their velocities υ_j and diffusion matrices $\tilde{D}$, and coupling constants λ_{ijk} needed for Eq. (10) in the main text.

2. Response functions in 4-mode regime

In this section, we derive the hydrodynamic model from the kinetics for the 4-mode regime. We start with the susceptibility matrix, that connects $\mathbf{q}$ and φ variables on the linear level. In this case, the set of zero modes of the collision integral is described by

$$\phi^T = T^{-1}(\mu_R,\ \mu_L, \upsilon, -1). \tag{D22}$$

Multiplying the distribution function by 1, p, ε_p and integrating over momentum, we find that for the right-moving electrons

$$\chi_4 = \frac{T}{2\pi}\begin{pmatrix} \frac{49\pi^4T^4}{24m^4u^9}+\frac{\pi^2T^2}{2m^2u^5}+\frac{1}{u} & 0 & m & -\frac{7\pi^4T^4}{6m^3u^7}-\frac{\pi^2T^2}{3mu^3} \\ 0 & \frac{49\pi^4T^4}{24m^4u^9}+\frac{\pi^2T^2}{2m^2u^5}+\frac{1}{u} & -m & \frac{7\pi^4T^4}{6m^3u^7}-\frac{\pi^2T^2}{3mu^3} \\ m & -m & -\frac{7\pi^4T^4}{12m^2u^7}+2m^2u-\frac{\pi^2T^2}{3u^3} & 0 \\ \frac{7\pi^4T^4}{6m^3u^7}+\frac{\pi^2T^2}{3mu^3} & \frac{7\pi^4T^4}{6m^3u^7}-\frac{\pi^2T^2}{3mu^3} & 0 & \frac{7\pi^4T^4}{5m^2u^5}+\frac{2\pi^2T^2}{3u} \end{pmatrix} \tag{D23}$$

and the matrix of currents

$$M_4 = ik\frac{T}{2\pi}\begin{pmatrix} 1 & 0 & -\frac{7\pi^4T^4}{24m^3u^7}-\frac{\pi^2T^2}{6mu^3}+mu & 0 \\ 0 & -1 & -\frac{7\pi^4T^4}{24m^3u^7}-\frac{\pi^2T^2}{6mu^3}+mu & 0 \\ -\frac{7\pi^4T^4}{24m^3u^7}-\frac{\pi^2T^2}{6mu^3}+mu & -\frac{7\pi^4T^4}{24m^3u^7}-\frac{\pi^2T^2}{6mu^3}+mu & 0 & \frac{7\pi^4T^4}{15m^2u^5}+\frac{2\pi^2T^2}{3u} \\ 0 & 0 & \frac{7\pi^4T^4}{15m^2u^5}+\frac{2\pi^2T^2}{3u} & 0 \end{pmatrix}. \tag{D24}$$

The rotating matrix

$$R_4 \simeq \frac{\sqrt{3u}}{2\pi^{3/2}T}\begin{pmatrix} mu^2 & -mu^2 & -u & 1 \\ -mu^2 & mu^2 & u & 1 \\ mu^2 & -mu^2 & -u & 1 \\ -mu^2 & mu^2 & u & 1 \end{pmatrix}. \tag{D25}$$

The velocities in this regime split linearly with temperature, in agreement with a general argument given in Ref. 92:

$$u_1 = -u + \frac{\pi T}{\sqrt{3mu}}, \tag{D26}$$

$$u_2 = u - \frac{\pi T}{\sqrt{3mu}}, \tag{D27}$$

$$u_3 = -u - \frac{\pi T}{\sqrt{3mu}}, \tag{D28}$$

$$u_4 = u + \frac{\pi T}{\sqrt{3mu}} \tag{D29}$$

We next compute the diffusion matrix

$$D_4 \simeq D_\varepsilon\begin{pmatrix} 0 & 0 & 0 & 0 \\ 0 & 0 & 0 & 0 \\ 0 & 0 & 0 & 0 \\ mu^2 & mu^2 & 0 & 1 \end{pmatrix}. \tag{D30}$$

Here, we have defined the energy diffusion constant $D_\varepsilon = u^6/l^4T^5$. After the rotation into an eigenmode basis $\tilde{D}_4 = R_4 D_4 R_4^{-1}$, one finds

$$\tilde{D}_4 \simeq \frac{3}{8\pi^2}D_\varepsilon\begin{pmatrix} 1 & 1 & 1 & 1 \\ 1 & 1 & 1 & 1 \\ 1 & 1 & 1 & 1 \\ 1 & 1 & 1 & 1 \end{pmatrix}. \tag{D31}$$

The density of the heat mode in the 4-mode regime is expressed in terms of hydrodynamic eigenmodes as

$$\varepsilon - \bar{w}(\rho_R - \rho_L) = \frac{T}{2}\sqrt{\frac{\pi}{3u}}(\Psi_1 + \Psi_2 + \Psi_3 + \Psi_4). \tag{D32}$$

All the coupling constants in this regime are of the same order

$$\lambda_1 = \frac{iTu^{3/2}\sqrt{3/\pi}}{4}\begin{pmatrix} 5 & -1 & 1 & -1 \\ -1 & -3 & 1 & -1 \\ 1 & 1 & 1 & 1 \\ -1 & -1 & 1 & -3 \end{pmatrix}, \tag{D33}$$

$$\lambda_2 = \frac{iTu^{3/2}\sqrt{3/\pi}}{4}\begin{pmatrix} 3 & 1 & 1 & -1 \\ 1 & -5 & 1 & -1 \\ 1 & 1 & 3 & -1 \\ -1 & -1 & -1 & -1 \end{pmatrix}, \tag{D34}$$

$$\lambda_3 = \frac{iTu^{3/2}\sqrt{3/\pi}}{4}\begin{pmatrix} 1 & 1 & 1 & 1 \\ 1 & -3 & -1 & -1 \\ 1 & -1 & 5 & -1 \\ 1 & -1 & -1 & -3 \end{pmatrix}, \tag{D35}$$

$$\lambda_4 = \frac{iTu^{3/2}\sqrt{3/\pi}}{4}\begin{pmatrix} 3 & -1 & 1 & 1 \\ -1 & -1 & -1 & -1 \\ 1 & -1 & 3 & 1 \\ 1 & -1 & 1 & -5 \end{pmatrix}. \tag{D36}$$

3. Response functions in 3-mode regime

In the three-mode regime, zero modes of the collision integral are given by

$$\phi^T = T^{\;1}(\mu, \upsilon, -1). \tag{D37}$$

The response function

$$\chi_3 = \frac{T}{\pi u}\begin{pmatrix} \frac{49\pi^4T^4}{24m^4u^8} + \frac{\pi^2T^2}{2m^2u^4} + 1 & 0 & -\frac{7\pi^4T^4}{6m^3u^6} - \frac{\pi^2T^2}{3mu^2} \\ 0 & -\frac{7\pi^4T^4}{24m^2u^6} + m^2u^2 - \frac{\pi^2T^2}{6u^2} & 0 \\ -\frac{\pi^2T^2}{3mu^2} & 0 & \frac{\pi^2T^2}{3} \end{pmatrix}. \tag{D38}$$

The dissipationless part of the current matrix is given by

$$M_3 = \frac{ikT}{\pi}\begin{pmatrix} 0 & -\frac{7\pi^4T^4}{24m^3u^7} - \frac{\pi^2T^2}{6mu^3} + mu & 0 \\ -\frac{7\pi^4T^4}{24m^3u^7} - \frac{\pi^2T^2}{6mu^3} + mu & 0 & \frac{7\pi^4T^4}{30m^2u^5} + \frac{\pi^2T^2}{3u} \\ 0 & \frac{7\pi^4T^4}{30m^2u^5} + \frac{\pi^2T^2}{3u} & 0 \end{pmatrix} \tag{D39}$$

The rotating matrix

$$R_3 \simeq \begin{pmatrix} -\frac{\pi^{3/2}T}{\sqrt{3}mu^{3/2}} & 0 & \frac{\sqrt{\frac{3}{\pi}}\sqrt{u}}{T} - \frac{\sqrt{3}\pi^{3/2}T}{2m^2u^{7/2}} \\ \sqrt{\frac{\pi}{2}}\sqrt{u} & -\frac{\sqrt{\frac{\pi}{2}}}{m\sqrt{u}} & \frac{\sqrt{2\pi}}{mu^{3/2}} \\ \sqrt{\frac{\pi}{2}}\sqrt{u} & \frac{\sqrt{\frac{\pi}{2}}}{m\sqrt{u}} & \frac{\sqrt{2\pi}}{mu^{3/2}} \end{pmatrix}. \tag{D40}$$

The velocities of the eigenmodes in the 3-mode regime are

$$u_1 = 0, \quad u_2 \simeq -u - \frac{\pi^2T^2}{3m^2u^3}, \quad u_3 \simeq u + \frac{\pi^2T^2}{3m^2u^3}. \tag{D41}$$

The heat current

$$\varepsilon - \bar{w}\rho = \sqrt{\frac{\pi}{3u}}T\Psi_1. \tag{D42}$$

The coupling constants

$$\lambda_1 = \begin{pmatrix} 0 & \frac{3i\sqrt{\frac{\pi}{2}}T^2}{m\sqrt{u}} & -\frac{3i\sqrt{\frac{\pi}{2}}T^2}{m\sqrt{u}} \\ \frac{3i\sqrt{\frac{\pi}{2}}T^2}{m\sqrt{u}} & \frac{i\sqrt{3}\pi^{3/2}T^3}{m^2u^{5/2}} & 0 \\ -\frac{3i\sqrt{\frac{\pi}{2}}T^2}{m\sqrt{u}} & 0 & -\frac{i\sqrt{3}\pi^{3/2}T^3}{m^2u^{5/2}} \end{pmatrix}, \tag{D43}$$

$$\lambda_2 = \begin{pmatrix} \frac{21i\sqrt{2}\pi^{5/2}T^4}{5m^3u^{9/2}} & \frac{7i\pi^{3/2}T^3}{2\sqrt{3}m^2u^{5/2}} & -\frac{7i\pi^{3/2}T^3}{2\sqrt{3}m^2u^{5/2}} \\ \frac{7i\pi^{3/2}T^3}{2\sqrt{3}m^2u^{5/2}} & \frac{7i\pi^{5/2}T^4}{30\sqrt{2}m^3u^{9/2}} & \frac{21i\pi^{5/2}T^4}{10\sqrt{2}m^3u^{9/2}} \\ -\frac{7i\pi^{3/2}T^3}{2\sqrt{3}m^2u^{5/2}} & \frac{21i\pi^{5/2}T^4}{10\sqrt{2}m^3u^{9/2}} & -\frac{133i\pi^{5/2}T^4}{30\sqrt{2}m^3u^{9/2}} \end{pmatrix}, \tag{D44}$$

$$\lambda_3 = \begin{pmatrix} -\frac{21i\sqrt{2}\pi^{5/2}T^4}{5m^3u^{9/2}} & \frac{7i\pi^{3/2}T^3}{2\sqrt{3}m^2u^{5/2}} & -\frac{7i\pi^{3/2}T^3}{2\sqrt{3}m^2u^{5/2}} \\ \frac{7i\pi^{3/2}T^3}{2\sqrt{3}m^2u^{5/2}} & \frac{133i\pi^{5/2}T^4}{30\sqrt{2}m^3u^{9/2}} & -\frac{21i\pi^{5/2}T^4}{10\sqrt{2}m^3u^{9/2}} \\ -\frac{7i\pi^{3/2}T^3}{2\sqrt{3}m^2u^{5/2}} & -\frac{21i\pi^{5/2}T^4}{10\sqrt{2}m^3u^{9/2}} & -\frac{7i\pi^{5/2}T^4}{30\sqrt{2}m^3u^{9/2}} \end{pmatrix}. \tag{D45}$$

Note that self-coupling of the heat mode vanishes

$$\lambda_{1,1,1} = 0. \tag{D46}$$

4. Pulses and their tails in fluctuating hydrodynamics

In this section we study the asymptotic form of the pulses in different regimes, analyzing the self-consistent mode-coupling equation. The results of this section are used in Eqs. (28), (29), and (30) of the main text. We start with the 4-mode regime.

4.1. 4-mode regime

To compute the asymptotic, we first analyze the impact of the interaction between the two modes. The "slow" mode propagates with velocities u_k and the "fast" mode moves a velocity u_l in the same direction. To be concrete, let us focus on the right (front) tail of the mode k. In the reference frame that moves with velocity u_k, the tail of this mode controlled by the coupling to the mode l is governed by the equation

$$\partial_t f_k(x, t) \simeq \frac{\lambda_{kll}^2}{T^5} \int_{\infty}^{\infty} dy \int_0^t ds f_k(x-y, t-s)\partial_y^2 f_l^2(y, s). \tag{D47}$$

Here, we omit the self-coupling and diffusion terms, which play no role far from the maximum. Due to the scale separation, this equation can be further simplified as follows:

$$\partial_t f_k(x, t) \simeq \frac{\lambda_{kll}^2}{T^2\lambda_{lll}^{2/3}} \partial_x^2 \int_0^t \frac{ds}{s^{2/3}} f_k(x - \Delta u_{kl}s, t - s). \tag{D48}$$

Here, we used the fact that the integration over spatial coordinates is limited to a region much smaller than the separation between the peaks, yielding $\int dy f_l^2(y, s) = \frac{T^3}{\lambda_{lll}^{2/3} s^{2/3}}$.

The slow mode can be approximated by its tail estimated at the peak of the fast mode. The latter is located at the point $y \sim \Delta u_{kl} s$. As distance x is smaller than the separation between the pulses $s\Delta u_{kl}$, one may neglect $s \sim x/(\Delta u_{kl})$ compared with t. Therefore, Eq. (D48) can be further simplified, yielding

$$\partial_t f_k(x, t) \simeq \frac{\lambda_{kll}^2}{\lambda_{lll}^{2/3}T^2} \partial_x^2 \int_0^t \frac{ds}{s^{2/3}} f_k(x - \Delta u_{kl}s, t - s). \tag{D49}$$

In the Fourier space, this reads

$$\partial_t f_k(q, t) = -\frac{\lambda_{kll}^2}{\lambda_{lll}^{2/3}T^2} q^2 \int_0^t \frac{ds}{s^{2/3}} e^{\quad ik\Delta u_{kl}s} f_k(q, s). \tag{D50}$$

Therefore one can look for a solution to the form

$$f_k(q, t) = Th(q^\gamma t). \tag{D51}$$

Plugging this anzats into Eq. (D50), one finds

$$h(z) \simeq \exp \quad -\frac{\lambda_{kll}^2 z}{\lambda_{lll}^{2/3} T^2 (\Delta u_{kl})^{1/3}}\Bigg). \tag{D52}$$

Fourier transforming back, we get the result for the tail of the mode f_k:

$$f_k(x, t) \simeq \frac{\lambda_{kll}^2 tx^{\quad (\gamma+1)}}{T\lambda_{lll}^{2/3}(\Delta u_{kl})^{1/3}}. \tag{D53}$$

Substituting $\gamma = 5/3$ and the values mode velocities and coupling constant, we finally find that modes propagating in the same direction mutually induce a tail that scales as

$$f_k(x, t) \sim (mu^7)^{1/3} tx^{\quad 8/3}, \tag{D54}$$

where x is the distance from the center of the peak. For each of the modes, the tail is on the side directed to the other mode. A similar analysis yields the tail between oppositely moving modes:

$$f_k(x, t) \sim (Tu^7)^{1/3} tx^{\quad 8/3}. \tag{D55}$$

4.2. 3-mode regime

We now apply similar arguments for the 3-mode regime. In this case, the tails of the static heat mode ($j = 1$) are governed by

Eq. (D53). Substituting the coupling constant for this regime, we find

$$f_1(x,t) \simeq \frac{T^{7/3}}{m^2 u^{7/3}} tx^{\ 8/3} \text{for } x \gg \left(\frac{T^4 t^3}{m^6 u^7}\right)^{1/5}. \quad \text{(D56)}$$

The rear tails of sound modes ($j = 2, 3$) in this regime are formed due to interaction between sound modes, with the result

$$f_{2/3}(x,t) \sim \frac{T^{13/3}}{m^4 u^{19/3}} tx^{\ 8/3}. \quad \text{(D57)}$$

5. Kubo formula in the hydrodynamic regime

Here, we review the Kubo formula approach for multicomponent fluid, focusing in more detail on the thermal conductivity. The starting point is that the fluid state assumes a local equilibrium, therefore the response function to external forces can be presented in the linear response formalism.[93,94] For multi-component fluid, this refers to the equilibration of the corresponding modes. For the brevity of notation, we suppress the chirality indexes and restore them when needed. In the presence of the external time-dependent perturbation $\widehat{V}$ the Hamiltonian of the fluid is given by

$$\widehat{H}(t) = \widehat{H}_0 + \widehat{V}(t) \quad \text{(D58)}$$

The perturbation can be expressed as time and space-dependent thermodynamic potentials

$$\widehat{V}(t) = -\int dx \left\{ \frac{\delta T(x,t)}{T}\left[\widehat{\varepsilon}(x,t) - \mu\widehat{\rho}(x,t)\right] + \delta\mu(x,\ t)\widehat{\rho}(x,\ t) + \upsilon(x,\ t)\widehat{g}(x,\ t). \right\} \quad \text{(D59)}$$

The expectation value of a generic operator J_i at a time t is given as an average with respect to the equilibrium density matrix:

$$\langle\hat{J}_i\rangle(t) = \frac{i}{\hbar}\int_{\infty}^{t} dt' \mathrm{Tr}\left\{\widehat{\rho}_0[\hat{V}^I(t'),\ \hat{J}_i^I(t)]\right\}. \quad \text{(D60)}$$

We now define the retarded current-current correlation function

$$K_{ij}(\omega,k) = \frac{i}{\hbar}\int_{\infty}^{\infty} dx \int_0^{\infty} dte^{\ ikx+i\omega t}\langle[\widehat{J}_i(x,t),\widehat{J}_j(0,0)]\rangle. \quad \text{(D61)}$$

By using (D60) one can show that linear-response coefficients L_{ij} can be expressed as

$$L_{ij}(k) = \frac{1}{-i\omega}\left[K_{ij}(\omega,k) - K_{ij}(\omega=0, k\to 0)\right]. \quad \text{(D62)}$$

The Kubo framework can be used for computing any linear response coefficients, and in particular thermal conductivity. To do it, one needs to define a thermal current. In a general many-body problem it can be computed by coupling the system to the gravitational field. For the fluid, this reduces to a much simpler expression[62]

$$\widehat{J}_T = \widehat{J}_E - \bar{w}\widehat{J}_\rho. \quad \text{(D63)}$$

Here, J_E and J_ρ are energy current and particle currents that are determined by energy conservation and particle conservation, $\bar{w} \simeq \pi^2 T^2/4mu^2$ is the enthalpy of the fluid per one electron (without the Fermi energy part). The Kubo formula for thermal conductivity reads

$$\sigma_T(\omega,k) = \frac{1}{i\omega T}\int_0^L dx \int_0^{\infty} dte^{\ ikx+i\omega t}\langle[\widehat{J}_T(x,t),\widehat{J}_T(0,0)]\rangle. \quad \text{(D64)}$$

Using the continuity equation for energy,

$$\frac{\partial\varepsilon}{\partial t} = -\mathrm{div}\ J_E, \quad \text{(D65)}$$

and particle number,

$$\frac{\partial\rho}{\partial t} = -\mathrm{div}\ J_\rho, \quad \text{(D66)}$$

one can express the heat-conductivity as

$$\sigma_T(\omega,k) = \frac{1}{T}\frac{\omega}{k^2}\langle[\widehat{\varepsilon} - \bar{w}\widehat{\rho}, \widehat{\varepsilon} - \bar{w}\widehat{\rho}\rangle^{\mathrm{ret}}_{\omega,k}. \quad \text{(D67)}$$

This can be cast in terms of the response function

$$\chi^{\mathrm{ret}}_{i,j}(x,t) = -i\theta(t)\langle[\widehat{\mathbf{q}}_i(x,t),\widehat{\mathbf{q}}_j(0,0)]\rangle. \quad \text{(D68)}$$

Specifically, for the four and three-mode regimes

$$\sigma_T(\omega,k) = \frac{i\omega}{k^2T^2}\left[\chi^{\mathrm{ret}}_{33}(\omega,k) + \bar{w}^2\chi^{\mathrm{ret}}_{33}(\omega,k) - 2\bar{w}\chi^{\mathrm{ret}}_{33}(\omega,k)\right]. \quad \text{(D69)}$$

5.1. Thermal conductivity in 4-mode regime

In this regime, the bare thermal conductivity is given by

$$\sigma_T(\omega=0,k) \sim \frac{\pi^2 T}{3ik} + \frac{u^5}{l^4T^4}. \quad \text{(D70)}$$

The imaginary (ballistic) part is protected by momentum conservation and therefore is unchanged, compared to the bare value computed within the kinetic theory (B16). The real part of the thermal conductivity is parametrically bigger. We now cast the Kubo formula in terms of Keldysh correlation functions, i.e. eigenmodes.

$$\sigma_T(\omega,k) = \frac{\pi^2\omega^2}{12uk^2}\sum_{j_1,j_2=1}^{4} f_{j_1,j_2}(\omega,k). \quad \text{(D71)}$$

This brings us back to the problem of pulse propagation we have extensively studied. Computed on the Gaussian level, this yields

$$\mathrm{Resigma}(\omega = 0, k) = \frac{\pi^2 T}{6u} \sum_{j_1, j_2 = 1}^{4} \tilde{D}_{j_1, j_2} \sim \frac{u^5}{l^4 T^4} \tag{D72}$$

in agreement with Eq. (D70).

We now take into account the self-renormalization effects, by employing Eq. (D71) with the pulse shape found from the self-consistent Eq. (8). Both the heads and tails of pulses are modified by interaction, and contribute to the thermal conductivity. The head of each pulse is governed by KPZ function $f(x, t) \simeq \frac{T^2}{(\lambda t)^{2/3}} f_{KPZ}\left(\frac{T(x\quad ut)}{(\lambda t)^{2/3}}\right)$.

This yields the contribution to thermal conductivity that scales with frequency as

$$\mathrm{Resigma}(\omega, k = 0) \sim \frac{\lambda^{4/3}}{Tu} \omega^{\quad 1/3} \simeq u T^{1/3} \omega^{\quad 1/3}. \tag{D73}$$

In addition, the tails of the distribution function (114) contribute

$$\mathrm{Resigma}(\omega, k) \sim (mu^4)^{1/3} k^{\quad 1/3}. \tag{D74}$$

Substituting $k = \omega/\Delta u$ one gets

$$\mathrm{Resigma}(\omega, k = 0) \sim u T^{1/3} \omega^{\quad 1/3}. \tag{D75}$$

Thus, we see that the contribution to the thermal conductivity from the head (D73) and the tails (D50) in the fourmode regime have the same order.

5.2 3-mode regime

The value of the thermal conductivity in the entire 3-mode regime is strongly renormalized by the interaction between the modes, so that its bare value has no significance. We thus express the conductivity via the pulse correlation functions

$$\sigma_T(\omega, k) = \frac{\pi^2 \omega^2}{12uk^2} f_1(\omega, k). \tag{D76}$$

Due to the lack of self-interaction, there is no anomalous peak broadening in the head of heat mode in the three-mode regime, and the thermal conductivity is determined solely by the tails of the pulse. Substitution of the asymptotics Eq. (D56) into Eq. (D76) yields

$$\mathrm{Resigma}(\omega, k) \sim \frac{T^2}{u^{10/3} m^2} k^{\quad 1/3}. \tag{D77}$$

Substituting $k = \omega/u$, we find

$$\mathrm{Resigma}(\omega, k = 0) \sim \frac{T^{7/3}}{u^3 m^2} \omega^{\quad 1/3}. \tag{D78}$$

REFERENCES

[1] R. N. Guzrhi, "Gidrodimamicheskie effekty v tverdyx telax pri nizkix temperaturax," Usp. Fiz. Nauk **94**, 689 (1968) [Hydrodynamic effects in solids at low temperature, Sov. Phys. Usp. **11**, 255 (1968)].

[2] D. A. Bandurin, I. Torre, R. K. Kumar, M. Ben Shalom, A. Tomadin, A. Principi, G. H. Auton, E. Khestanova, K. S. Novoselov, I. V. Grigorieva, L. A. Ponomarenko, A. K. Geim, and M. Polini, "Negative local resistance caused by viscous electron backflow in graphene," Science **351**, 1055 (2016).

[3] A. D. Levin, G. M. Gusev, E. V. Levinson, Z. D. Kvon, and A. K. Bakarov, "Vorticity-induced negative nonlocal resistance in a viscous two-dimensional electron system," Phys. Rev. B **97**, 245308 (2018).

[4] D. A. Bandurin, A. V. Shytov, L. S. Levitov, R. K. Kumar, A. I. Berdyugin, M. Ben Shalom, I. V. Grigorieva, A. K. Geim, and G. Falkovich, "Fluidity onset in graphene," Nat. Commun. **9**, 4533 (2018).

[5] A. I. Berdyugin, S. G. Xu, F. M. D. Pellegrino, R. Krishna Kumar, A. Principi, I. Torre, M. Ben Shalom, T. Taniguchi, K. Watanabe, I. V. Grigorieva, M. Polini, A. K. Geim, and D. A. Bandurin, "Measuring Hall viscosity of graphene's electron fluid," Science **364**, 162 (2019).

[6] M. Kim, S. G. Xu, A. I. Berdyugin, A. Principi, S. Slizovskiy, N. Xin, P. Kumaravadivel, W. Kuang, M. Hamer, R. Krishna Kumar, R. V. Gorbachev, K. Watanabe, T. Taniguchi, I. V. Grigorieva, V. I. Falko, M. Polini, and A. K. Geim, "Control of electron-electron interaction in graphene by proximity screening," Nat. Commun. **11**, 2339 (2020).

[7] A. Gupta, J. J. Heremans, G. Kataria, M. Chandra, S. Fallahi, G. C. Gardner, and M. J. Manfra, "*Hydrodynamic and ballistic transport over large length scales in* GaAs/AlGaAs," Phys. Rev. Lett. **126**, 076803 (2021).

[8] J. A. Sulpizio, L. Ella, A. Rozen, J. Birkbeck, D. J. Perello, D. Dutta, M. Ben-Shalom, T. Taniguchi, K. Watanabe, T. Holder, R. Queiroz, A. Principi, A. Stern, T. Scaffidi, A. K. Geim, and S. Ilani, "Visualizing poiseuille flow of hydrodynamic electrons," Nature **576**, 75 (2019).

[9] M. J. H. Ku, T. X. Zhou, Q. Li, Y. J. Shin, J. K. Shi, C. Burch, L. E. Anderson, A. T. Pierce, Y. Xie, A. Hamo, U. Vool, H. Zhang, F. Casola, T. Taniguchi, K. Watanabe, M. M. Fogler, P. Kim, A. Yacoby, and R. L. Walsworth, "Imaging viscous flow of the dirac fluid in graphene," Nature **583**, 537 (2020).

[10] A. Jenkins, S. Baumann, H. Zhou, S. A. Meynell, D. Yang, K. Watanabe, T. Taniguchi, A. Lucas, A. F. Young, and A. C. B. Jayich, "Imaging the breakdown of ohmic transport in graphene," Phys. Rev. Lett. **129**, 087701 (2022).

[11] U. Vool, A. Hamo, G. Varnavides, Y. Wang, T. X. Zhou, N. Kumar, Y. Dovzhenko, Z. Qiu, C. A. C. Garcia, A. T. Pierce, J. Gooth, P. Anikeeva, C. Felser, P. Narang, and A. Yacoby, "Imaging phonon mediated hydrodynamic flow in WTe_2", Nat. Phys. **17**, 1216 (2021).

[12] J. Crossno, J. K. Shi, K. Wang, X. Liu, A. Harzheim, A. Lucas, S. Sachdev, P. Kim, T. Taniguchi, K. Watanabe, T. A. Ohki, and K. C. Fong, "Observation of the dirac fluid and the breakdown of the wiedemann–franz law in graphene," Science **351**, 1058 (2016).

[13] J. Gooth, F. Menges, N. Kumar, V. Süβ, C. Shekhar, Y. Sun, U. Drechsler, R. Zierold, C. Felser, and B. Gotsmann, "Thermal and electrical signatures of a hydrodynamic electron fluid in tungsten diphosphide," Nat. Commun. **9**, 4093 (2018).

[14] O. E. Raichev, G. M. Gusev, A. D. Levin, and A. K. Bakarov, "Manifestations of classical size effect and electronic viscosity in the magnetoresistance of narrow two-dimensional conductors: Theory and experiment," Phys. Rev. B **101**, 235314 (2020).

[15] D. Taubert, G. J. Schinner, C. Tomaras, H. P. Tranitz, W. Wegscheider, and S. Ludwig, "An electron jet pump: The venturi effect of a Fermi liquid," J. Appl. Phys. **109**, 102412 (2011).

[16] P. J. W. Moll, P. Kushwaha, N. Nandi, B. Schmidt, and A. P. Mackenzie, "Evidence for hydrodynamic electron flow in $PdCoO_2$," Science **351**, 1061 (2016).

[17] R. Krishna Kumar, D. A. Bandurin, F. M. D. Pellegrino, Y. Cao, A. Principi, H. Guo, G. H. Auton, M. Ben Shalom, L. A. Ponomarenko, G. Falkovich, K. Watanabe, T. Taniguchi, I. V. Grigorieva, L. S. Levitov, M. Polini, and

A. K. Geim, "Superballistic flow of viscous electron fluid through graphene constrictions," Nat. Phys. **13**, 1182 (2017).
[18]B. A. Braem, F. M. D. Pellegrino, A. Principi, M. Rsli, C. Gold, S. Hennel, J. V. Koski, M. Berl, W. Dietsche, W. Wegscheider, M. Polini, T. Ihn, and K. Ensslin, "Scanning gate microscopy in a viscous electron fluid," Phys. Rev. B **98**, 241304 (2018).
[19]G. M. Gusev, A. S. Jaroshevich, A. D. Levin, Z. D. Kvon, and A. K. Bakarov, "Stokes flow around an obstacle in viscous two-dimensional electron liquid," Sci. Rep. **10**, 7860 (2020).
[20]G. M. Gusev, A. S. Jaroshevich, A. D. Levin, Z. D. Kvon, and A. K. Bakarov, "Viscous magnetotransport and gurzhi effect in bilayer electron system," Phys. Rev. B **103**, 075303 (2021).
[21]Z. J. Krebs, W. A. Behn, S. Li, K. J. Smith, K. Watanabe, T. Taniguchi, A. Levchenko, and V. W. Brar, "Imaging the breaking of electrostatic dams in graphene for ballistic and viscous fluids," Science **379**, 671 (2023).
[22]J. Geurs, Y. Kim, K. Watanabe, T. Taniguchi, P. Moon, and J. H. Smet, "Rectification by hydrodynamic flow in an encapsulated graphene tesla valve," arXiv:2008.04862 (2020).
[23]S. Samaddar, J. Strasdas, K. Janßen, S. Just, T. Johnsen, Z. Wang, B. Uzlu, S. Li, D. Neumaier, M. Liebmann, and M. Morgenstern, "Evidence for local spots of viscous electron flow in graphene at moderate mobility," Nano Lett. **21**, 9365 (2021).
[24]C. Kumar, J. Birkbeck, J. A. Sulpizio, D. J. Perello, T. Taniguchi, K. Watanabe, O. Reuven, T. Scaffidi, A. Stern, A. K. Geim, and S. Ilani, "Imaging hydrodynamic electrons flowing without landauer–sharvin resistance," Nature **609**, 276 (2022).
[25]K. A. Matveev and A. V. Andreev, "Hybrid sound modes in one-dimensional quantum liquids," Phys. Rev. Lett. **121**, 026803 (2018).
[26]K. A. Matveev and A. V. Andreev, "Two-fluid dynamics of one-dimensional quantum liquids in the absence of galilean invariance," Phys. Rev. B **100**, 035418 (2019).
[27]B. Bertini, M. Collura, J. De Nardis, and M. Fagotti, "Transport in out-of-equilibrium XXZ chains: Exact profiles of charges and currents," Phys. Rev. Lett. **117**, 207201 (2016).
[28]O. A. Castro-Alvaredo, B. Doyon, and T. Yoshimura, "Emergent hydrodynamics in integrable quantum systems out of equilibrium," Phys. Rev. X **6**, 041065 (2016).
[29]V. B. Bulchandani, R. Vasseur, C. Karrasch, and J. E. Moore, "Bethe-Boltzmann hydrodynamics and spin transport in the XXZ chain," Phys. Rev. B **97**, 045407 (2018).
[30]B. Doyon, "Lecture notes on generalised hydrodynamics," SciPost Phys. Lect. Notes **18** (2020).
[31]B. Bertini, F. Heidrich-Meisner, C. Karrasch, T. Prosen, R. Steinigeweg, and M. Žnidarič, "Finite-temperature transport in one-dimensional quantum lattice models," Rev. Mod. Phys. **93**, 025003 (2021).
[32]A. F. Andreev, "The hydrodynamics of two and one dimensional liquids," Sov. Phys. JETP **51**, 1038 (1980).
[33]K. Schwab, E. Henriksen, J. Worlock, and M. Roukes, "Measurement of the quantum of thermal conductance," Nature **404**, 974 (2000).
[34]M. Meschke, W. Guichard, and J. P. Pekola, "Singlemode heat conduction by photons," Nature **444**, 187 (2006).
[35]S. Jezouin, F. D. Parmentier, A. Anthore, *et al.*, "Quantum limit of heat flow across a single electronic channel," Science **342**, 601 (2013).
[36]L. Cui, W. Jeong, S. Hur, *et al.*, "Quantized thermal transport in single-atom junctions," Science **355**, 1192 (2017).
[37]E. Sivre, A. Anthore, F. D. Parmentier, A. Cavanna, U. Gennser, A. Ouerghi, Y. Jin, and F. Pierre, "Heat Coulomb blockade of one ballistic channel," Nature **14**, 145 (2018).
[38]C. Altimiras, H. le Sueur, U. Gennser, A. Anthore, A. Cavanna, D. Mailly, and F. Pierre, "Energy relaxation in the integer quantum Hall regime," Phys. Rev. Lett. **109**, 026803 (2012).
[39]V. Venkatachalam, S. Hart, L. Pfeiffer, K. West, and A. Yacoby, "Local thermometry of neutral modes on the quantum Hall edge," Nat. Phys. **8**, 676 (2012).
[40]H. Inoue, A. Grivnin, Y. Ronen, M. Heiblum, V. Umansky, and D. Mahalu, "Proliferation of neutral modes in fractional quantum Hall states," Nat. Comm. **5**, 4067 (2014).
[41]I. V. Protopopov, D. B. Gutman, M. Oldenburg, and A. D. Mirlin, "Dissipationless kinetics of one-dimensional interacting fermions," Phys. Rev. B **89**, 161104 (2014).
[42]I. V. Protopopov, D. B. Gutman, P. Schmitteckert, and A. D. Mirlin, "Dynamics of waves in 1D electron systems: Density oscillations driven by population inversion," Phys. Rev. B **87**, 045112 (2013).
[43]A. Imambekov and L. I. Glazman, "Universal theory of nonlinear luttinger liquids," Science **323**, 228 (2009); "Phenomenology of one-dimensional quantum liquids beyond the low-energy limit," Phys. Rev. Lett. **102**, 126405 (2009).
[44]A. Imambekov, T. L. Schmidt, and L. I. Glazman, "One-dimensional quantum liquids: Beyond the luttinger liquid paradigm," Rev. Mod. Phys. **84**, 1253 (2012).
[45]M. Khodas, M. Pustilnik, A. Kamenev, and L. I. Glazman, "Fermi-Luttinger liquid: Spectral function of interacting one-dimensional fermions," Phys. Rev. B **76**, 155402 (2007).
[46]M. Schick, "Flux quantization in a one-dimensional model," Phys. Rev. **166**, 404 (1968).
[47]F. D. M. Haldane, "Luttinger liquid theory of one-dimensional quantum fluids," J. Physics C **14**, 2585 (1981).
[48]B. Sakita, *Quantum Theory of Many-Variable Systems and Fields* (Wolrd Scientific, Singapore, 1985).
[49]A. Jevicki and B. Sakita, "The quantum collective field method and its application to the planar limit, Nuc," Phys. B **165**, 511 (1980).
[50]I. V. Protopopov, D. B. Gutman and A. D. Mirlin, "relaxation in luttinger liquids: Bose–Fermi duality." Phys. Rev. B **90**, 125113 (2014).
[51]A. V. Rozhkov, Phys. Rev. B **77**, 125109 (2008); Phys. Rev. B **74**, 245123 (2006); Eur. Phys. J. **47**, 193 (2005).
[52]M. Stone, *Bosonization* (World Scientific, 1994).
[53]J. von Delft and H. Schoeller, "Bosonization for beginners-refermionization for experts," Annalen Phys. **7**, 225 (1998).
[54]R. Samanta, I. V. Protopopov, A. D. Mirlin, and D. B. Gutman, "Thermal transport in one-dimensional electronic fluid," Phys. Rev. Lett. **122**, 206801 (2019).
[55]I. V. Protopopov, R. Samanta, A. D. Mirlin, and D. B. Gutman, "Anomalous hydrodynamics in one-dimensional electronic fluid," Phys. Rev. Lett. **126**, 256801 (2021).
[56]A. M. Lunde, K. Flensberg, and L. I. Glazman, Phys. Rev. B **75**, 245418 (2007).
[57]K. A. Matveev and A. V. Andreev, "Equilibration of a spinless luttinger liquid," Phys. Rev. B **85**, 041102 (2012).
[58]T. Micklitz, J. Rech, and K. A. Matveev, "Transport properties of partially equilibrated quantum wires," Phys. Rev. B **81**, 115313 (2010).
[59]K. A. Matveev and A. V. Andreev, "Scattering of hole excitations in a one-dimensional spinless quantum liquid," Phys. Rev. B **86**, 045136 (2012).
[60]C. L. Kane and M. P. A. Fisher, "Thermal transport in a luttinger liquid," Phys. Rev. Lett. **76**, 3192 (1996).
[61]A. Levchenko, T. Micklitz, J. Rech, and K. A. Matveev, "Transport in partially equilibrated inhomogeneous quantum wires," Phys. Rev. B **82**, 115413 (2010).
[62]J. M. Luttinger, "Theory of thermal transport coefficients," Phys. Rev. **135**, A1505 (1964).
[63]C. Castellani, G. Kotliar, and P. A. Lee, "Fermi-liquid theory of interacting disordered systems and the scaling theory of the metal-insulator transition," Phys. Rev. Lett. **59**, 323 (1987).
[64]H. Spohn, Fluctuating hydrodynamics approach to equilibrium time correlations for anharmonic chains, in: edited by, S. Lepri, *Thermal Transport in Low Dimensions: From Statistical Physics to Nanoscale Heat Transfer., Lect. Not. Phys.* (Springer, 2016), p. 107. arXiv:1505.05987.
[65]H. Spohn, "Nonlinear fluctuating hydrodynamics for anharmonic chains," J. Stat. Phys. **154**, 1191–1227 (2014).
[66]M. Kulkarni and A. Lamacraft, "From GPE to KPZ: Finite temperature dynamical structure factor of the 1D bose gas," Phys. Rev. A **88**, 021603 (2013).

[67]V. B. Bulchandani, S. Gopalakrishnan, and E. Ilievski, "Superdiffusion in spin chains," J. Stat. Mech. **2021**, 084001 (2021).
[68]M. Ljubotina, M. Žnidarič and T. Prosen, "Spin diffusion from an inhomogeneous quench in an integrable system," Nat. Commun. **8**, 16117 (2017).
[69]M. Ljubotina, M. Žnidarič, and T. Prosen, "Kardar-Parisi-Zhang physics in the quantum heisenberg magnet," Phys. Rev. Lett. **122**, 210602 (2019).
[70]A. Scheie, N. E. Sherman, M. Dupont, S. E. Nagler, M. B. Stone, G. E. Granroth, J. E. Moore, and D. A. Tennant, "Detection of kardar–parisi–zhang hydrodynamics in a quantum heisenberg spin-1/2 chain," Nat. Phys. **17**, 726 (2021).
[71]D. Wei, A. Rubio-Abadal, B. Ye, F. Machado, J. Kemp, K. Srakaew, S. Hollerith, J. Rui, S. Gopalakrishnan, N. Y. Yao, I. Bloch, and J. Zeiher, "Quantum gas microscopy of kardar–parisi–zhang superdiffusion," Science **376**, 716 (2022).
[72]P. N. Jepsen, J. Amato-Grill, I. Dimitrova, W. W. Ho, E. Demler, and W. Ketterle, "Spin transport in a tunable heisenberg model realized with ultracold atoms," Nature **588**, 403 (2020).
[73]H. van Beijeren, "Exact results for anomalous transport in one-dimensional Hamiltonian systems," Phys. Rev. Lett. **108**, 180601 (2012).
[74]M. Prahofer, Exact scaling functions for one-dimensional stationary KPZ growth, http://www-m5.ma.tum.de/KPZ.
[75]M. Prahofer and H. Spohn, "Exact scaling functions for one dimensional stationary KPZ growth," J. Stat. Phys. **115**, 255 (2004).
[76]E. Fermi, J. Pasta, S. Ulam, and M. Tsingou, *Studies of non-Linear Problems, FPU*, Document LA-1940. Los Alamos National Laboratory (1955).
[77]T. Mai, A. Dhar, and O. Narayan, "Equilibration and universal heat conduction in Fermi–pasta–ulam chains," Phys. Rev. Lett. **98**, 184301 (2007).
[78]A. Pereverzev, "*Fermi–pasta–ulam β lattice: Peierls equation and anomalous heat conductivity*, phys," Rev. E **68**, 056124 (2003).
[79]H. Spohn and J. Lukkarinen, "Anomalous energy transport in the FPU-β chain," Commun. Pure Appl. Math. **61**, 1753 (2008).
[80]V. V. Uchaikin and V. M. Zolotarev, *Chance and Stability, Stable Distributions and Their Applications* (W. de Gruyter, Berlin, 1999).
[81]M. Arzamasovs, F. Bovo, and D. M. Gangardt, "Kinetics of mobile impurities and correlation functions in one-dimensional superfluids at finite temperature," Phys. Rev. Lett. **112**, 170602 (2014).
[82]K. Samokhin, "Lifetime of excitations in a clean luttinger liquid," J. Phys.: Condens. Matter **10**, 533 (1998).
[83]O. Narayan and S. Ramaswamy, "Anomalous heat conduction in one-dimensional momentum-conserving systems," Phys. Rev. Lett. **89**, 200601 (2002).
[84]T. Giamarchi, *Quantum Physics in One Dimension* (Clarendon Press, Oxford, 2004).
[85]A. O. Gogolin, A. A. Nersesyan, and A. M. Tsvelik, *Bosonization in Strongly Correlated Systems* (University Press, Cambridge, 1998).
[86]A. Kamenev, *Field Theory of Non Equilibrium Systems* (Cambridge University Press, Cambridge, 2011).
[87]J. Rammer and H. Smith, "Quantum field-theoretical methods in transport theory of metals," Rev. Mod. Phys. **58**, 323 (1986).
[88]J. Lin, K. A. Matveev, and M. Pustilnik, "Thermalization of acoustic excitations in a strongly interacting one-dimensional quantum liquid," Phys. Rev. Lett. **110**, 016401 (2013).
[89]The fermionic quasiparticles introduced in this way are advantageous over the original electrons of the model because their interaction vanishes in the low-energy limit. In particular, they have flat density of states at the Fermi surface. There is a similarity between the composite fermions defined in the Bose–Fermi Duality[50] and exact quasiparticle computed within Bethe ansatz solutions (and used in the GHD framework).
[90]L. D. Landau and E. M. Lifshitz, *Statistical Physics* (Elsevier, Oxford, 1990).
[91]K. A. Matveev, "Sound in a system of chiral one dimensional fermions," Phys. Rev. B **102**, 155401 (2020).
[92]K. A. Matveev and A. V. Andreev, "Hybrid sound modes in one-dimensional quantum liquids," Phys. Rev. Lett. **121**, 026803 (2018).
[93]L. Kadanoff and P. Martin, "Hydrodynamic equations and correlation functions," Ann. Phys. **24**, 419 (1963).
[94]P. Kovtun, "*Lectures on hydrodynamic fluctuations in relativistic theories*," J, Phys. A **45**, 473001 (2012).